

になるかもしれない。

## VI. siRNAの*in vivo*へのデリバリー

siRNAは細胞質でRISCに取り込まれて切断活性を発揮することより、siRNAのデリバリーは細胞膜さえ越えればよく、遺伝子治療によく使われる発現DNAベクターのように核にアクセスする必要がない。McCaffrey<sup>15)</sup>らはマウスの尾静脈から10~50 $\mu$ gの合成siRNAを体重の5~10%の大量のPBS溶液で5~7秒の短時間で注入するハイドロダイナミクス法で、マウス肝細胞へのsiRNAの導入に成功した。さらに最近、このハイドロダイナミクス法で導入されたFas<sup>16)</sup>やCaspase-8に対する合成siRNAが、マウスにおいて誘発された劇症肝炎による死亡率を低下させたことが報告され、siRNAが*in vivo*でも有効であることが示された。またマウスにおいて、siRNAは脳血管関門があるため中枢神経系には入らないが、肝臓のほか腎臓、脾臓、肺、膵臓に導入可能であることが報告されている<sup>17)</sup>。だがヒトでは、臓器組織への圧力と循環系への用量負荷のため、そのまま臨床応用することは難しい。最近、siRNAのセンス鎖の3'末端にコレステロールを結合させることにより、通常の方法の静脈注射でも肝臓と腸管への導入が可能であることが示された<sup>18)</sup>。その他、有効なカチオニックリポソームベクターが開発されており、これらについては和田氏や平林氏の稿を参照されたい。

長期の抑制効果にはウイルスベクターが必要となる。shRNA発現ベクターコンストラクトをアデノウイルスやレンチウイルス、レトロウイルス、アデノ随伴ウイルスなどのウイルスベクターに組み込んで作製したsiRNA発現ウイルスベクターを用いて、*in vivo*の細胞へのsiRNA導入の報告が次々とされている<sup>19)</sup>。特に最近開発されたアデノ随伴ウイルスの新しい血清型は非常に高い遺伝子導入効率があり期待されている。

しかし、これらのいずれの方法でも静脈注射などの全身性の投与でsiRNAを脳血管関門を越えて中枢神経系にデリバリーすることは困難で、siRNAによる神経変性疾患治療の大きな問題になっている。最近筆者らは脳血管内皮細胞へのsiRNAの導入に成功した。脳血管障害、多発性硬化症への応用が期待される。

## おわりに

siRNAの核酸医薬としての臨床応用の研究には、上記以外にもサイレンシングの突然の停止の問題(シャットダウン現象)など解決すべき課題はまだ多くある。しかし、基礎研究は爆発的に進んでおり、最も大きな問題であるデリバリー方法にも急速な進歩がある。非常に近い将来に、難治性疾患での新しい治療法の開発にsiRNAが利用が突破口になると期待している。

## 文献

- 1) Amarzguiou M, et al: Nucleic Acids Res (2003) 31: 589-595
- 2) Jackson AL, et al: Nat Biotechnol (2003) 21: 635-637
- 3) Bridge AJ, et al: Nat Genet (2003) 34: 263-264
- 4) Yokota T, et al: EMBO Rep (2003) 4: 602-608
- 5) Garrus JE, et al: Cell (2001) 107: 55-65
- 6) Surabhi RM, et al: J Virol (2002) 76: 12963-12973
- 7) Arteaga HJ, et al: Nat Biotechnol (2003) 21: 230-231
- 8) Sorensen DR, et al: J Mol Biol (2003) 327: 761-766
- 9) Xia H, et al: Nat Med (2004) 10: 816-820
- 10) Yokota T, et al: Biochem Biophys Res Commun (2004) 314: 283-291
- 11) Gonzalez-Alegre P, et al: Ann Neurol (2003) 53: 781-787
- 12) Miller VM, et al: Proc Natl Acad Sci USA (2003) 100: 7195-7200
- 13) Li Y, et al: Ann Neurol (2004) 56: 124-129
- 14) Kao SC, et al: Biol Chem (2004) 279: 1942-1949
- 15) McCaffrey AP, et al: Nature (2002) 418: 38-39
- 16) Song E, et al: Nat Med (2003) 9: 347-351
- 17) Lewis DL, et al: Nat Genet (2002) 32: 107-108
- 18) Soutschek J, et al: Nature (2004) 432: 173-178
- 19) Davidson B, et al: Lancet Neurol (2004) 3: 145-149

## for beginners

- ・「改訂RNAi実験プロトコール」多比良和誠ら 編: 羊土社 (2004)
- ・“RNAi”グレゴリー・ハノン 編, 中村義一 日本語版監修: メディカル・サイエンス・インターナショナル (2004)

# Atorvastatin Attenuates Remnant Lipoprotein-Induced Monocyte Adhesion to Vascular Endothelium Under Flow Conditions

Akio Kawakami, Akira Tanaka, Katsuyuki Nakajima, Kentaro Shimokado, Masayuki Yoshida

**Abstract**—Remnant lipoproteins have been reported to play a causative role in atherogenesis. We investigated the effect of remnant-like lipoprotein particles (RLPs) on monocyte-endothelial interaction and their potential regulation by atorvastatin. Monocytic U937 cells were incubated with RLPs isolated from hypertriglyceridemia subjects and their adhesion to human umbilical vein endothelial cells (HUVECs) was examined under flow conditions. Incubation of U937 cells with 15  $\mu$ g protein/mL RLPs increased their adhesion to HUVECs activated with IL-1 $\beta$  (untreated:  $6.8 \pm 1.6$  cells/HPF versus RLPs:  $16.2 \pm 3.3$  cells/HPF,  $P < 0.05$ ). Flow cytometric analysis revealed that incubation with RLPs increased expression levels of CD11a, CD18, and CD49d in U937 cells. Moreover, RLP-induced RhoA activation as well as FAK activation was seen in U937 cells, and RLP-induced RhoA activation seemed to be involved with PKC-dependent signaling. To explore the effect of atorvastatin on RLP-induced U937 cell adhesion to HUVECs, U937 cells were incubated with RLPs in the presence of atorvastatin. Pretreatment of U937 cells with 10  $\mu$ mol/L atorvastatin significantly decreased RLP-induced U937 cell adhesion to activated HUVECs (RLP  $15.2 \pm 1.5$  cells/HPF versus atorvastatin+RLP  $10.2 \pm 1.0$  cells/HPF;  $P < 0.05$ ) and decreased the enhanced integrin expression in RLP-treated U937 cells. Atorvastatin also inhibited RLP-induced RhoA activation and FAK activation in U937 cells. In summary, RLPs induced monocyte adhesion to vascular endothelium by sequential activation of PKC, RhoA, FAK, and integrins, indicating a role of remnant lipoproteins in vascular inflammation during atherogenesis. Atorvastatin attenuated this enhanced monocyte adhesion to HUVECs, suggesting an antiinflammatory role for this compound. (*Circ Res.* 2002;91:263-271.)

**Key Words:** remnant-like lipoprotein particles ■ monocyte adhesion ■ atherosclerosis  
■ 3-hydroxyl-3-methylglutaryl coenzyme A reductase inhibitor

Hypercholesterolemia is regarded as a major risk factor of ischemic heart diseases, and modified low-density lipoprotein (LDL) has been reported to contribute to early atherosclerotic lesion formation. However, recent studies have reported that elevated serum triglyceride was observed in patients with coronary artery disease without marked hypercholesterolemia, and that serum triglyceride may be a risk factor of ischemic heart disease.<sup>1</sup> Remnant lipoproteins, produced by hydrolysis of chylomicron (CM), and very low-density lipoprotein (VLDL) are considered to be atherogenic triglyceride-rich lipoproteins (TRLs). Indeed, clinical studies have revealed that remnant lipoproteins are closely related to atherosclerosis, independent of LDL.<sup>2</sup> There is also increasing evidence that remnant lipoproteins play a causative role in atherogenesis, as a previous report has shown that remnant-like lipoprotein particles (RLPs) induced vascular smooth muscle cell proliferation.<sup>3</sup> However, the cellular

mechanisms of RLPs in atherogenesis have not been fully elucidated.

Monocyte adhesion to vascular endothelium plays an important role in atherogenesis<sup>4</sup> and another report showed that RLPs increased the expression levels of adhesion molecules on endothelial cells.<sup>5</sup> In the present study, we investigated the direct effects of RLPs on monocytes and subsequent monocyte-endothelial interactions under flow conditions, along with the mechanisms involved in cell surface integrin expression, actin cytoskeleton, and inside-out signal transduction.

3-hydroxyl-3-methylglutaryl coenzyme A (HMG-CoA) reductase inhibitor, or statin, has been suggested to have beneficial effects for the prevention of atherosclerosis,<sup>6</sup> independent of its LDL-cholesterol lowering effect. We recently found that statin modulated the actin cytoskeleton, downregulated integrins in monocytes, and decreased monocyte adhe-

Original received August 29, 2001; resubmission received January 8, 2002; revised resubmission received June 21, 2002; accepted June 24, 2002.  
From the Department of Medical Biochemistry (A.K., M.Y.), Graduate School of Medicine, and the Department of Geriatric Medicine (A.K., A.T., K.S., M.Y.), Tokyo Medical and Dental University; and Japan Immunoresearch Laboratories (K.N.), Tokyo, Japan.  
Correspondence to Masayuki Yoshida, MD, Dept of Medical Biochemistry, Graduate School of Medicine, Tokyo Medical and Dental University, 1-5-45, Yushima, Bldg. D-621, Bunkyo-ku, Tokyo 113-8510 Japan. E-mail masa.vasc@tmd.ac.jp  
© 2002 American Heart Association, Inc.

sion to endothelial cells.<sup>6</sup> Thus, in the present study, we attempted to determine whether atorvastatin modifies the effect of RLPs on monocytes.

## Materials and Methods

### Cell Culture and Reagents

U937 and THP-1 cell lines obtained from American Type Culture Collection, Manassas, Va, and human umbilical vein endothelial cells (HUVECs) isolated from normal-term umbilical cords were cultured as described previously.<sup>6</sup> C3 exoenzyme was obtained from Wako, Japan. Human recombinant apolipoprotein (apo) E<sub>3</sub>, mevalonic acid, and cytochalasin D were obtained from Sigma-Aldrich, Japan. Calphostin C and phorbol-12-myristate-13-acetate (PMA) were obtained from Calbiochem, Germany. FITC-conjugated phalloidin was obtained from Molecular Probes. Atorvastatin calcium hydrate, monocalcium bis [(3R,5R)-7-[2-(4-fluorophenyl)-5-isopropyl-3-phenyl-4-phenylcarbamoyl-1H-pyrrol-1-yl]-3,5-dihydroxyheptanoate] trihydrate was a gift from Pfizer Inc, Groton, Conn. An RLP-C Kit was a gift from Japan Immunoresearch Laboratories, Tokyo, Japan. Antibodies used in the present study were as follows: mouse anti-CD11a monoclonal antibody (clone 38, Ancell Corp), mouse anti-CD11b monoclonal antibody (clone 44, YLEM, Italy), mouse anti-CD18 monoclonal antibody (clone MEM48, Southern Biotechnology Associates), mouse anti-CD49d monoclonal antibody (clone A4-PUJ1, Upstate Biotechnology), mouse anti-L-selectin monoclonal antibody (clone FMC46, Serotec, UK), mouse anti-RhoA monoclonal antibody (Santa Cruz Biotechnology), mouse anti-focal adhesion kinase (FAK) polyclonal and anti-phosphorylated (p)FAK (397Y) polyclonal antibodies (Biosource), mouse anti- $\beta_1$ -integrin antibody (HUTS21) (PharMingen), mouse anti- $\beta_1$ -integrin antibody (7B4R) (Santa Cruz Biotechnology), mouse anti-PKC $\alpha$ , - $\beta$ , - $\gamma$ , - $\delta$ , - $\epsilon$  monoclonal antibodies (New England Biolabs), and HRP-conjugated goat anti-mouse IgG and FITC-conjugated goat anti-mouse IgG antibodies (Cal-tag). To examine cell viability, U937 cells were stained with a 0.25% trypan blue solution after incubation with RLPs or atorvastatin.

### Lipoprotein Preparation

EDTA plasma was obtained from 24 patients with hypertriglyceridemia who showed an elevated RLP-cholesterol concentration [ $>0.19$  mmol cholesterol/L (7.5 mg cholesterol/dL)],<sup>7</sup> 4 hours after their breakfast [8 kcal/kg standard weight (carbohydrate 62%; fat 17%; protein 21%)]. They had no cardiovascular diseases or diabetes and had not taken cardiovascular medicine or antioxidants. The protocol of this study complies with the guidelines for the conduct of research involving human subjects by the Committee on Human Research at the Tokyo Medical and Dental University. Total TRLs ( $d<1.006$ ) was isolated by density gradient ultracentrifugation from plasma samples. RLPs were isolated from plasma samples using an RLP-C Kit, as described previously.<sup>7</sup> TRLs (total TRL) and RLPs were then dialyzed overnight against 5 liters of PBS containing 50  $\mu$ mol/L EDTA (pH 7.4), and then sterilized using a 0.22- $\mu$ m filter unit (Millipore). The protein concentration of lipoprotein was determined by a modified method of Lowry et al.<sup>7a</sup> The lipid fraction was extracted from purified lipoproteins (TRL and RLP) or U937 cells using chloroform and methanol, dried under N<sub>2</sub> gas, and stored in dimethylsulfoxide before use. Degraded RLPs were prepared by repeated freezing and thawing.<sup>8</sup> Trypsinized (tryp-) RLPs, devoid of immunochemically detectable apo E, were prepared as described previously.<sup>9</sup> The cholesterol patterns of TRLs and RLPs were selectively detected by sensitive high-performance liquid chromatography (HPLC). Ten microgram proteins of TRLs and RLPs were analyzed by SDS-PAGE in a 5% to 20% linear gradient gel (Funakoshi), and visualized with a silver stain reagent (Daiichi, Japan). Lipid compositions of the lipoproteins (TRL and RLP) or U937 cell lipid extracts were measured enzymatically by SRL, Japan.

### Monocyte Adhesion Assay

The protocols of the adhesion assay under static and flow conditions have been previously described in detail.<sup>6</sup> For the flow assays, HUVEC monolayers were stimulated with 10 U/mL IL-1 $\beta$  (Genzyme) for 4 hours on coverslips and then positioned in a flow chamber mounted on an inverted microscope (IX70, Olympus, Japan). HUVEC monolayers were perfused for 5 minutes with perfusion medium, and then U937 cells ( $1 \times 10^6$ /mL) were drawn through the chamber with a syringe pump (PHD2000, Harvard Apparatus) for 10 minutes at a controlled flow rate to generate a shear stress of 1.0 dyne/cm<sup>2</sup>. The entire period of perfusion was recorded on videotape, and then transferred to a personal computer for image analysis to determine the number of rolling and adherent U937 cells on HUVEC monolayers in 10 randomly selected 20 $\times$  microscope fields.

### Integrin Expression in U937 Cells

U937 cells ( $1 \times 10^6$ /mL) were treated with the indicated primary antibodies for 45 minutes on ice, washed twice with RPMI-1640 and 5% FCS, and incubated with FITC-conjugated goat anti-mouse antibody. Fluorescent intensity was analyzed using a FACS Caliber (Becton-Dickinson).<sup>10</sup>

### Quantitation of Filamentous Actin in U937 Cells

Filamentous actin (F-actin) in U937 cells was quantitated as described previously.<sup>6</sup> In brief, U937 cells ( $1 \times 10^6$ /mL) were fixed with 1% paraformaldehyde for 5 minutes, permeabilized with 0.1% Triton X-100 for 60 seconds, and incubated with FITC-conjugated phalloidin for 60 minutes. Fluorescent intensity of the U937 cells was quantitated using a fluorescent plate reader and also observed using a fluorescent microscope.

### Translocation of RhoA and PKC in U937 Cells

To examine the translocation of RhoA and PKC from the cytosol to the membrane, membrane and total cell lysates of U937 cells ( $1 \times 10^6$ /mL) were prepared as described previously.<sup>6,11</sup> An equal amount of protein (10  $\mu$ g) from each fraction was subjected to 12.5% SDS-PAGE, and then Western blotting analysis was performed using anti-RhoA monoclonal antibody and monoclonal antibodies to the indicated PKC isoforms. Immunoreactive RhoA and PKC protein was detected with an enhanced chemiluminescence (ECL) kit (Amersham Pharmacia Biotech).

### Phosphorylation of FAK in U937 Cells

A total cell lysate of U937 cells ( $1 \times 10^6$ /mL) was prepared as described above, and Western blotting analysis was performed using anti-pFAK(397Y) and anti-FAK antibodies. Immunoreactive pFAK and FAK proteins were detected with an ECL kit.

### Antisense Treatment

FAK antisense oligonucleotides (5'-ATAATCCAGCTGAACCAAG-3'), sense oligonucleotides (5'-CTTGGTTCAAGCTGGATTAT-3'), and mismatch sense oligonucleotides (5'-ATAATCGACGTTCAAGCAAG-3'), selected from the human FAK gene (GenBank accession No. L13616), were synthesized with a phosphorothioate modification by Sawady Technology, Japan. THP-1 cells were suspended in 6-well plates ( $2 \times 10^6$ /well) for 24 hours, and 750  $\mu$ L of OptiMem (Life Technologies) containing 12  $\mu$ L of Lipofectin (Life Technologies)/2  $\mu$ g oligonucleotide was added. After 5 hours, 1500  $\mu$ L of culture medium was added to THP-1 cells. An adhesion assay using transfected THP-1 cells was performed 24 hours after transfection.

### Statistical Analysis

Results are presented as mean  $\pm$  SD. Data were analyzed using analysis of variance (ANOVA), with a value of  $P < 0.05$  considered significant.

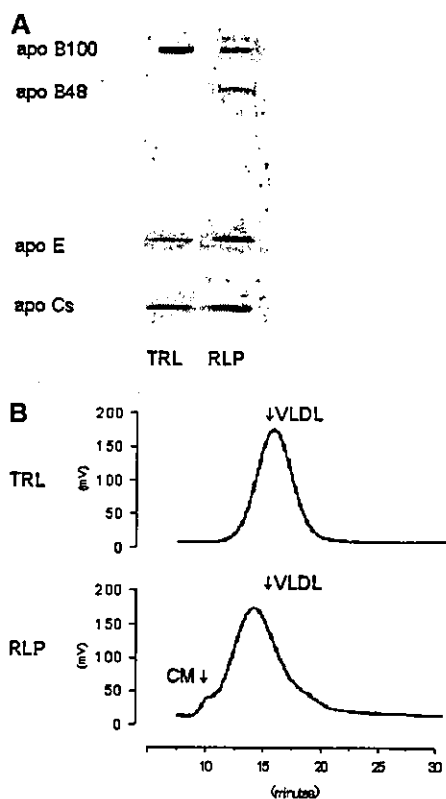


**Figure 1.** Characterization of lipoproteins. A, Apolipoprotein compositions of TRLs and RLPs. Protein (10  $\mu$ g) from TRLs and RLPs was analyzed by SDS-PAGE in 5% to 20% linear gradient gels and then visualized with silver stain reagent. Data are representative of 5 separate experiments. B, Particle sizes of TRLs and RLPs from hypertriglyceridemia subjects. Cholesterol patterns of TRLs and RLPs (20  $\mu$ g protein/mL) were selectively detected by HPLC. Identification of the cholesterol peak was made by comparison to the cholesterol standard. Data are representative of 4 separate experiments.

## Results

### Characterization of Lipoproteins

An SDS-PAGE analysis showed that the TRLs consisted of particles containing apo E and apo B-100. RLPs were found to be enriched in apo E, and contained apo B-100 as well as a small amount of apo B-48. Apo A-I was not detected (Figure 1A). HPLC analysis showed that RLPs consisted mainly of lipoproteins with particle sizes in the range of VLDL and some in the range of CM. TRLs consisted of lipoproteins with particle sizes in the typical range of VLDL (Figure 1B). Taken together, the prepared RLPs consisted of VLDL remnants and a small amount of CM remnants, as reported previously,<sup>12</sup> while TRLs were composed of nascent VLDL. SDS-PAGE analysis showed that tryp-RLPs had a trace of apo E (data not shown). HPLC showed that degraded RLPs had lost peaks of CM- and VLDL-cholesterol (data not shown). As shown in Table 1, lipid compositions were not significantly different between TRLs and RLPs.

### RLPs Induce U937 Cell Adhesion to HUVECs

U937 cells were incubated with various concentrations of TRLs or RLPs for 48 hours, after which static adhesion assays were performed. Adhesion of RLP-treated U937 cells

**TABLE 1.** Lipid Compositions of TRL and RLP

	TRL	RLP	P
Triglyceride	68.78 $\pm$ 2.56	63.10 $\pm$ 2.50	NS
Fatty acids	0.03 $\pm$ 0.02	0.03 $\pm$ 0.02	NS
Cholesterol ester	6.44 $\pm$ 1.18	8.32 $\pm$ 1.89	NS
Free cholesterol	6.08 $\pm$ 0.88	5.99 $\pm$ 1.05	NS
Phospholipid	18.68 $\pm$ 0.51	21.55 $\pm$ 0.64	NS

TRL indicates triglyceride-rich lipoproteins; RLP, remnant-like lipoprotein particles.

Data are from 5 separate experiments. Values (weight %) are presented as mean $\pm$ SD.

to HUVECs was significantly increased in a concentration-dependent manner (Figure 2A). The effect was observed with as little as 15  $\mu$ g protein/mL, which corresponded to 7.5 mg cholesterol/dL, and with this concentration, the adhesion of U937 cells was significantly increased under static conditions with as little as 18 hours of preincubation (data not shown). In contrast, incubation with TRLs had no effect on the adhesion of U937 cells to HUVECs (data not shown). Thus, we chose to incubate U937 cells with 15  $\mu$ g protein/mL RLPs for 18 hours in the following experiments.

Because RLPs consist of several lipid components and apolipoproteins, we considered it important to elucidate which of these components play a primary role in enhanced U937 cell adhesion. As shown in Figure 2B, RLP lipid extract, degraded RLPs, and tryp-RLPs all failed to induce a comparable level of U937 cell adhesion to HUVECs as native RLPs. Incubation with apo E, the most abundant apolipoprotein found in RLPs, also did not affect U937 cell adhesion.

The effect of RLPs on monocyte-endothelial interaction was next examined under flow conditions (shear stress of 1.0 dyne/cm<sup>2</sup>). When U937 cells were incubated with RLPs, adhesion of U937 cells to activated HUVECs was significantly increased compared with medium alone (control) (Figure 2C). In contrast, the number of rolling U937 cells on activated HUVECs was not significantly affected by RLPs. Incubation with TRLs did not affect either the rolling or adhesion of U937 cells (Figure 2C).

The effect of atorvastatin on RLP-induced monocyte-endothelial interaction was also examined. U937 cells were pretreated with various concentrations of atorvastatin for 48 hours before the addition of RLPs. RLP-induced U937 cell adhesion to activated HUVECs was reduced in a concentration-dependent manner with up to 10  $\mu$ mol/L atorvastatin. The inhibitory effect of atorvastatin was abrogated by the coinubation with 10  $\mu$ mol/L mevalonic acid, which metabolically bypasses the effect of atorvastatin (Figure 2D). With this concentration, RLP-induced U937 cell adhesion was reduced after 24 hours of preincubation and reached a plateau after 48 hours (data not shown). Similar results were obtained under static conditions (data not shown). Thus, we chose to pretreat U937 cells with 10  $\mu$ mol/L atorvastatin for 48 hours in the following experiments.

### Lipid Content of U937 Cells Treated With RLPs

To evaluate the potential role of lipid uptake by U937 cells in the observed adhesive interaction, U937 cells were incubated

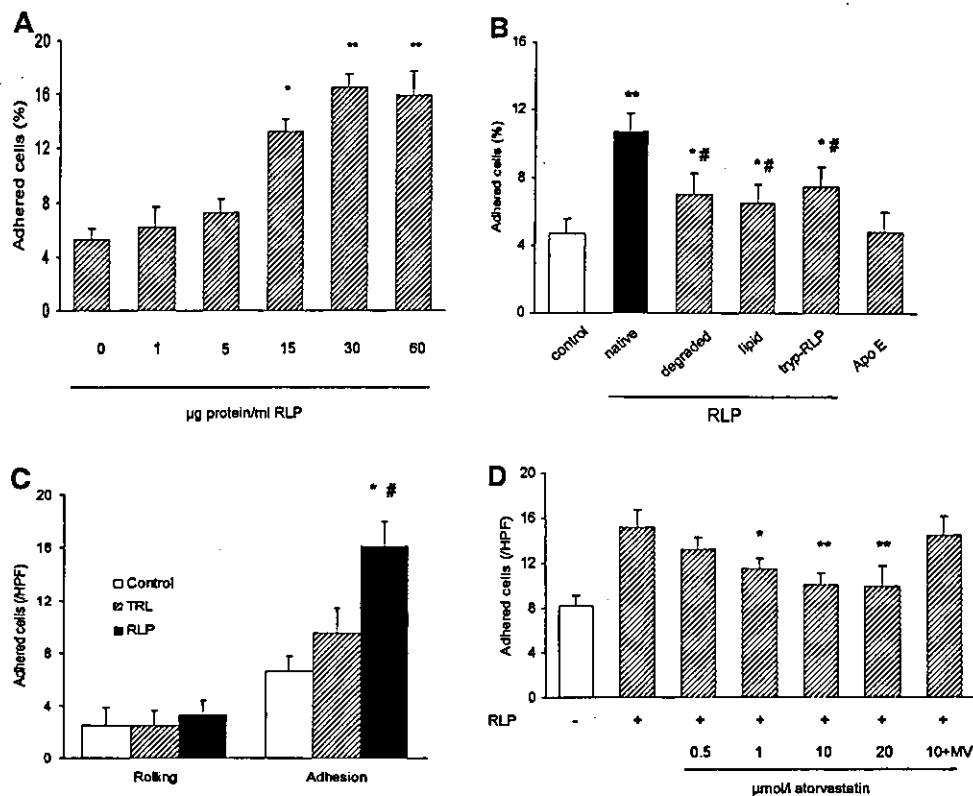


**Figure 2.** Effects of RLPs and atorvastatin on adhesion of U937 cells to HUVECs. **A**, U937 cells ( $2 \times 10^6$ /mL) were incubated with various concentrations of RLPs for 48 hours, and a static adhesion assay to HUVEC monolayers was performed. Data are from 4 separate experiments. \* $P < 0.05$ , \*\* $P < 0.01$  vs 0  $\mu\text{g}$  protein/mL RLPs. **B**, U937 cells ( $2 \times 10^6$ /mL) were incubated with native RLPs (15  $\mu\text{g}$  protein/mL), RLP lipid extract (7.5 mg cholesterol/dL), degraded RLPs (15  $\mu\text{g}$  protein/mL), tryp-RLPs (15  $\mu\text{g}$  protein/mL), apo E (15  $\mu\text{g}$ /mL), or medium alone (control) for 18 hours, and a static adhesion assay to HUVEC monolayers was performed for each condition. Data are from 3 separate experiments. \* $P < 0.05$ , \*\* $P < 0.01$  vs control; # $P < 0.05$  vs RLPs. **C**, U937 cells ( $1 \times 10^6$ /mL) were incubated with 15  $\mu\text{g}$  protein/mL RLPs (RLP), 15  $\mu\text{g}$  protein/mL TRLs (TRL), or medium alone (control) for 18 hours, and then perfused over HUVEC monolayers activated with 10 U/mL IL-1 $\beta$  for 4 hours with a shear stress of 1.0 dyne/cm $^2$ . Rolling and adherent U937 cells on HUVEC monolayers were counted under 20 $\times$  microscope fields for 10 minutes as described in Materials and Methods. Data are from 4 separate experiments. \* $P < 0.05$  vs control; # $P < 0.05$  vs TRLs. **D**, U937 cells ( $1 \times 10^6$ /mL) were pretreated with various concentrations of atorvastatin for 48 hours and then incubated with 15  $\mu\text{g}$  protein/mL RLPs for 18 hours, after which an adhesion assay to activated HUVEC monolayers were performed under flow conditions (1.0 dyne/cm $^2$ ). In some condition, U937 cells were pretreated with 10  $\mu\text{mol/L}$  atorvastatin and 10  $\mu\text{mol/L}$  mevalonic acid (10+MV). Data are from 4 separate experiments. \*\* $P < 0.01$  vs RLP(-); # $P < 0.05$  vs RLP(+).

as described in Figure 2, and then intracellular cholesterol ester (CE) and triglyceride (TG) concentrations were measured (Table 2). When U937 cells were treated with RLPs, these lipid concentrations were significantly increased as compared with the medium alone (control). Further, lipid concentrations of U937 cells treated with degraded RLPs and tryp-RLPs were significantly lower than those treated with native RLPs. Pretreatment of U937 cells with atorvastatin (atr+RLP) did not significantly alter the increase of CE and TG in RLP-treated U937 cells.

### RLPs Induce Integrin Expression on U937 Cells

To elucidate the molecular mechanism(s) of RLP-induced U937 cell adhesion, U937 cell surface integrin expression was examined by flow cytometric analysis. As shown in Figure 3A, when U937 cells were incubated with RLPs, the expressions of CD11a, CD18, and CD49d in U937 cells were increased, and when pretreated with atorvastatin, RLP-induced integrin expression was attenuated. In contrast, the expressions of CD11b and L-selectin on U937 cells, relatively low at baseline, were not affected by RLPs or atorvastatin (Figure 3A). Further, TRLs did

**TABLE 2. Lipid Content in U937 Cells Treated With Lipoproteins**

	Control	TRL	RLP	tryp-RLP	Degraded RLP	atr+RLP
Triglyceride	10.0 $\pm$ 2.3	35.2 $\pm$ 4.6*	98.5 $\pm$ 16.1**	40.5 $\pm$ 9.9**	30.2 $\pm$ 13.2**	90.0 $\pm$ 34.1
CE	0.5 $\pm$ 0.2	2.5 $\pm$ 1.2*	6.7 $\pm$ 1.4**	2.8 $\pm$ 1.8#	2.1 $\pm$ 0.8**	4.5 $\pm$ 1.5

CE indicates cholesterol ester; TRL, triglyceride-rich lipoproteins; RLP, remnant-like lipoprotein particles; and atr, atorvastatin.

Data are from 5 separate experiments. Values ( $\mu\text{g}/\text{mg}$  cell protein) are presented as mean $\pm$ SD. \* $P < 0.05$  vs control; \*\* $P < 0.01$  vs control; # $P < 0.05$  vs RLP; ## $P < 0.01$  vs RLP.

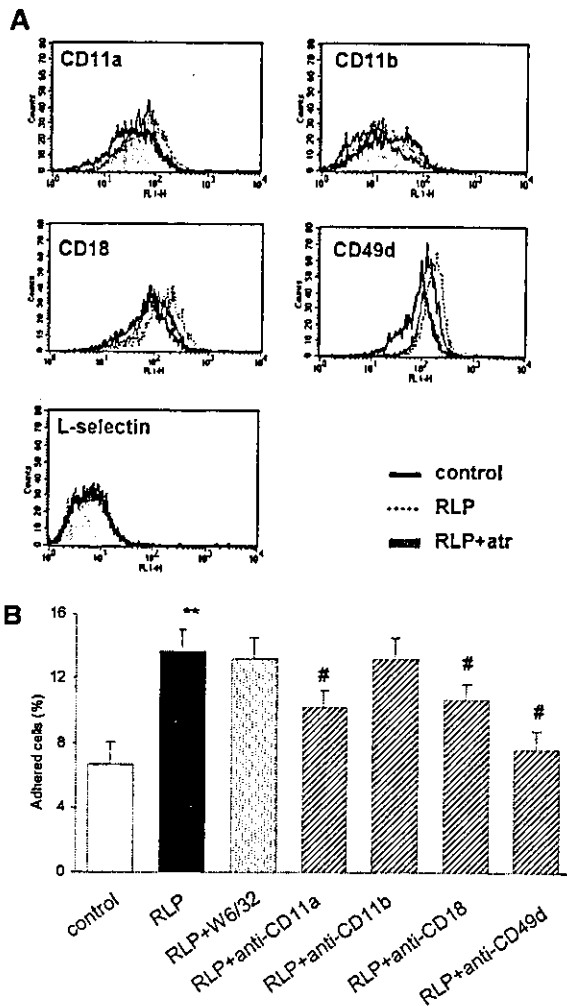


**Figure 3.** Effects of RLPs and atorvastatin on integrin expression in U937 cells. **A**, U937 cells ( $1 \times 10^6/\text{mL}$ ) were incubated in the presence of  $15 \mu\text{g}$  protein/mL RLPs (RLP) or medium alone (control) for 18 hours, or pretreated with  $10 \mu\text{mol/L}$  atorvastatin (RLP+atr) for 48 hours before incubation with RLPs. Expression levels of integrins in U937 cells were analyzed by a flow cytometric analysis using monoclonal antibodies to CD11a, CD11b, CD18, CD49d, and L-selectin for each condition. Five thousands cells were analyzed. Data are representative of 4 separate experiments. **B**, Effect of antibodies to integrins on RLP-induced U937 cell adhesion under static conditions. RLP-treated U937 cells ( $2 \times 10^6/\text{mL}$ ) were incubated with antibodies to the indicated integrins for 45 minutes and a static adhesion assay to HUVEC monolayers was performed. Data are from 4 separate experiments. \*\* $P < 0.01$  vs control; # $P < 0.05$  vs RLP.

not have any effect on integrin expression (data not shown). To examine whether the integrins were functionally correlated with RLP-induced U937 cell adhesion, RLP-treated U937 cells were incubated in the presence of antibodies to the integrins for 45 minutes and static adhesion assays were performed. Treatment with the anti-CD49d antibody significantly decreased RLP-induced U937 cell adhesion. Treatment with the anti-CD11a and anti-CD18 antibodies also reduced U937 cell adhesion, though less significantly (Figure 3B).

#### RLPs Induce Actin Polymerization in U937 Cells

The effect of RLPs on actin cytoskeleton organization in U937 cells was examined by detecting F-actin. Observation

under a fluorescent microscope showed morphologically abundant F-actin in RLP-treated U937 cells (Figure 4A), whereas TRLs had no effect on the actin cytoskeleton (data not shown). When U937 cells were preincubated with atorvastatin, the increase in F-actin induced by RLPs was significantly smaller as compared with RLPs alone (Figure 4A). RLP-induced U937 cell adhesion was significantly reduced after 10 minutes of pretreatment with  $1 \mu\text{g}/\text{mL}$  cytochalasin D, a specific inhibitor of actin polymerization (Figure 4C).

#### RLPs Induce RhoA Activation in U937 Cells

The effect of RLPs on RhoA activation in U937 cells was investigated by examining the translocation of RhoA from the cytoplasm to the membrane. Western blotting analysis revealed that the expression level of RhoA protein in the membrane fraction was significantly increased after incubation with RLPs (Figure 4B); however, it was not affected by TRLs (data not shown). In contrast, when U937 cells were pretreated with atorvastatin, RLP-induced RhoA translocation in U937 cells was significantly inhibited (Figure 4B). RLP-induced U937 cell adhesion was significantly reduced by 48 hours of pretreatment with  $30 \mu\text{g}/\text{mL}$  C3 exoenzyme, a specific inhibitor of RhoA (Figure 4C).

#### RLPs Induce FAK Activation in U937 Cells

The effect of RLPs on FAK activation in U937 cells was also investigated. Western blotting analysis using antibodies to pFAK(397Y) revealed that activated FAK was significantly increased after incubation with RLPs (Figure 5A). When U937 cells were pretreated with C3 exoenzyme or cytochalasin D, RLP-induced FAK activation was significantly decreased. Further, pretreatment with atorvastatin also caused a similar reduction of FAK activation (Figure 5A). Incubation with TRLs did not affect FAK activation in U937 cells (data not shown). To examine the functional significance of FAK in monocyte-endothelial interaction, we performed a static adhesion assay using THP-1 cells transfected with FAK antisense oligonucleotides to inhibit the FAK function. FAK protein expression in THP-1 cells transfected with FAK antisense was significantly reduced (Figure 5B), and the amount of adhesion to HUVECs was also greatly reduced as compared with those transfected with sense or mismatch sense oligonucleotides, whereas RLP treatment failed to induce adhesion to HUVECs in FAK antisense-transfected THP-1 cells (Figure 5C). To investigate the involvement of FAK in integrin activation, Western blotting analysis was performed using HUTS21 to detect the activation-dependent epitope of  $\beta_1$ -integrin in THP-1 cells transfected with FAK sense or FAK antisense. Activated  $\beta_1$ -integrin was significantly increased after incubation with RLPs in THP-1 cells transfected with FAK sense, but not with FAK antisense (Figure 5D).

#### RLPs Induce PKC Activation in U937 Cells

The involvement of PKC in RLP-induced U937 cell adhesion was investigated. To monitor PKC activation, the translocation of PKC from the cytoplasm to the membrane was examined. Western blotting analysis revealed that the expression levels of PKC $\alpha$ , PKC $\beta$ , and PKC $\delta$  proteins in the

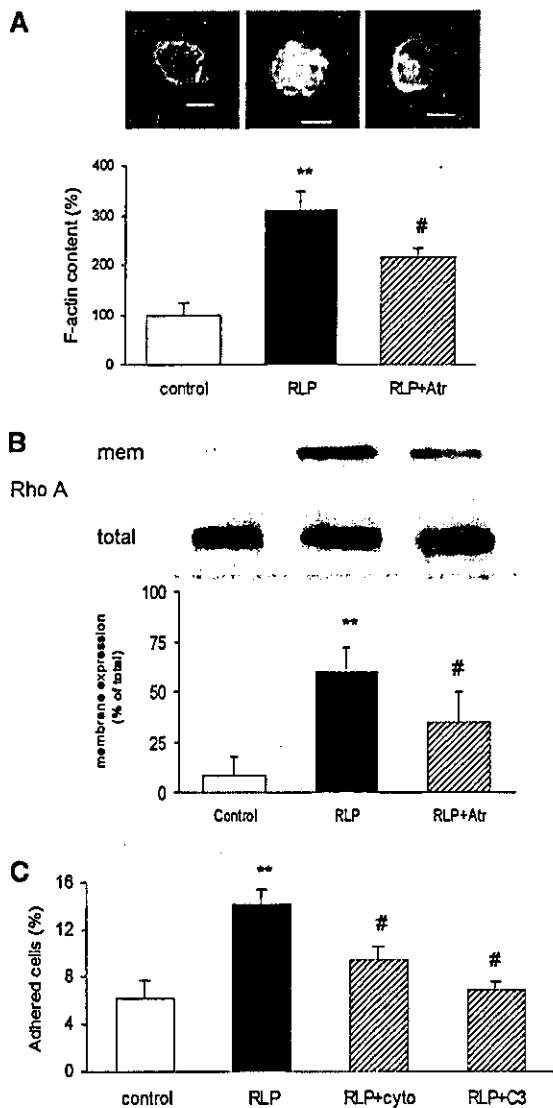


**Figure 4.** Effects of RLP and atorvastatin on actin polymerization and RhoA activation in U937 cells. **A**, U937 cells ( $1 \times 10^6$ /mL) were incubated in the presence of  $15 \mu\text{g}$  protein/mL RLPs (RLP) or medium alone (control) for 18 hours, or pretreated with  $10 \mu\text{mol/L}$  atorvastatin (RLP+atr) for 48 hours before incubation with RLPs. F-actin in U937 cells detected with FITC-conjugated phalloidin was observed under a fluorescent microscope, quantitated using a fluorescent plate reader, and expressed as a percentage to that of the control U937 cells. Photos are representative of 3 separate observations. Bars in the photos correspond to  $5 \mu\text{m}$ . Data are from 4 separate experiments. \*\* $P < 0.01$  vs control; # $P < 0.05$  vs RLPs. **B**, U937 cells ( $1 \times 10^6$ /mL) were incubated as described in **A**. RhoA expression was detected in the membrane (mem) and total lysate of U937 cells ( $1 \times 10^6$ /mL) for each condition by Western blotting ( $10 \mu\text{g}$  protein/lane). Blots are representative of 3 separate experiments. Bar graph shows the ratio of membrane RhoA expression to total RhoA expression from 4 separate experiments. \*\* $P < 0.01$  vs control; # $P < 0.05$  vs RLPs. **C**, U937 cells ( $1 \times 10^6$ /mL) were incubated in the presence of  $15 \mu\text{g}$  protein/mL RLPs (RLP) or medium alone (control) for 18 hours, or pretreated with  $1 \mu\text{g/mL}$  cytochalasin D (RLP+cyto) for 10 minutes or  $30 \mu\text{g/mL}$  C3 exoenzyme (RLP+C3) for 48 hours before incubation with RLPs. Static adhesion assay to HUVEC monolayers was performed for each condition. Data are from 4 separate experiments. \*\* $P < 0.01$  vs control; # $P < 0.05$  vs RLPs.

membrane were significantly increased after incubation with RLPs, although they were not affected by C3 exoenzyme (Figure 6A). PKC activation was not induced by incubation with TRLs (data not shown) and pretreatment of U937 cells with atorvastatin did not affect RLP-induced PKC activation (data not shown). When U937 cells were pretreated with  $5 \mu\text{mol/L}$  PMA for 18 hours, to deplete intracellular active PKC, or for 18 hours with  $2.5 \mu\text{mol/L}$  calphostin C, a specific PKC inhibitor, RLP-induced RhoA activation and U937 cell adhesion were significantly inhibited (Figures 6B and 6C).

## Discussion

We investigated the effects of remnant lipoproteins on the adhesion of monocytes to vascular endothelium under flow conditions. Incubation of U937 cells, a monocytic cell line, with pathophysiological concentrations of RLPs [ $>0.19$  mmol cholesterol/L ( $7.5$  mg cholesterol/dL)] significantly increased their adhesion to HUVECs under flow conditions. The level of laminar shear stress ( $1.0$  dyne/cm<sup>2</sup>) adopted for the present study has been observed physiologically at the points of bifurcation in large vessels, which are known to be atherosclerosis prone sites.<sup>6</sup> In contrast, TRLs, which mainly consist of nascent VLDL, had little effect on monocyte-endothelial interaction. These results indicate that elevated levels of remnant lipoproteins may have a causative role in the development of atherosclerosis through monocyte recruitment on vascular endothelium.

We demonstrated that the surface expression levels of integrins (CD11a, CD18, and CD49d) in U937 cells were increased after incubation with RLPs; however, the relatively modest quantitative upregulation of these integrins might not be adequate for the observed induction of U937 cell adhesion to HUVECs by RLPs. Therefore, we investigated the effects of RLPs on the relevant intracellular mechanism(s) of U937 cells that may modulate monocyte-endothelial interactions. First, we examined the effects of RLPs on the actin cytoskeleton and RhoA of U937 cells, because the actin cytoskeleton anchored to adhesion sites is known to be correlated with monocyte adhesion to vascular endothelium and migration, and RhoA is one of the most important molecules regulating the actin cytoskeleton.<sup>13</sup> The observed effects of RLPs on RhoA activation and cytoskeleton modulation shed light on a novel intracellular mechanism by which RLPs induce monocyte adhesion.

It is also known that FAK regulates cell adhesion and migration in various cell types, including nonadherent blood cells, by transferring signals to integrins at the cellular adhesion site.<sup>14</sup> FAK is autophosphorylated at 397Y flanked by the  $\beta_1$ -integrin binding site, which results in its enhanced kinase activity.<sup>15</sup> We showed that the phosphorylation of FAK at 397Y was increased after incubation with RLPs, and that the transfection of FAK antisense resulted in a reduction of RLP-induced U937 cell adhesion. Inhibition of RhoA activity reduced FAK phosphorylation. We also demonstrated that RLP-induced  $\beta_1$  integrin activation was dependent on FAK. Taken together, these results indicate that RLP treatment induced RhoA activation and subsequently activated FAK, eventually enhancing monocyte adhesion via integrin affinity modulation.

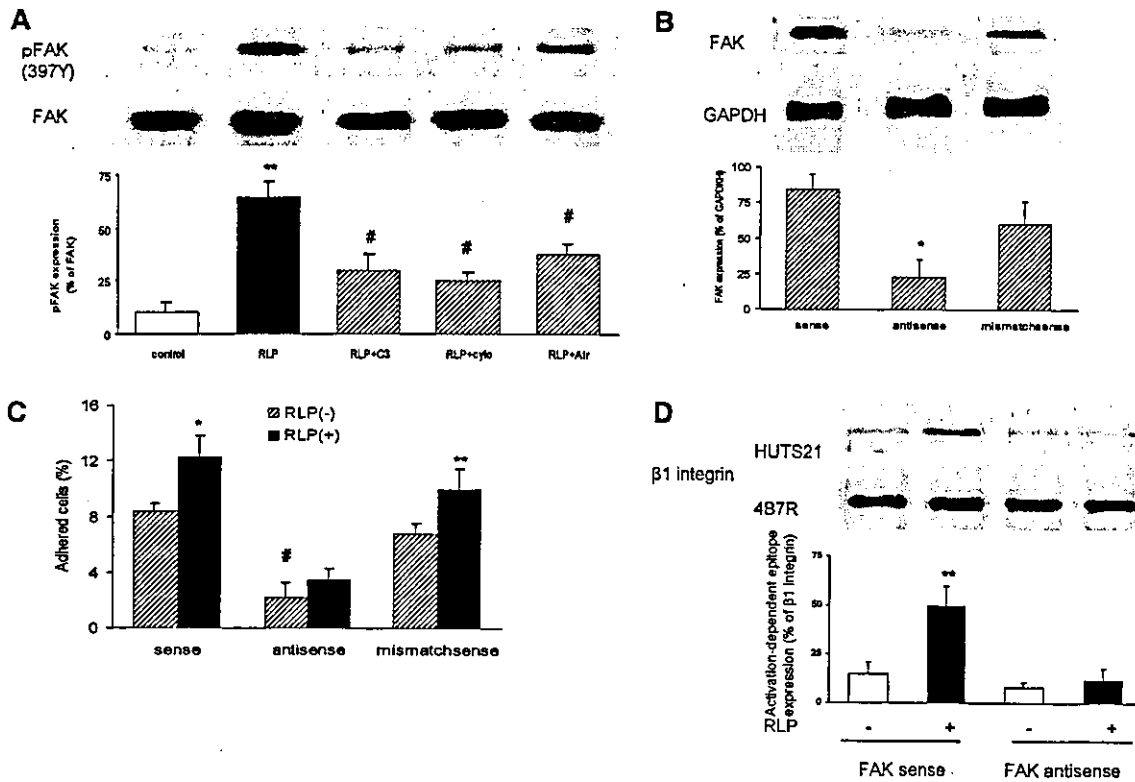


**Figure 5.** Effects of RLPs and atorvastatin on FAK activation in U937 cells. **A**, U937 cells ( $1 \times 10^6$ /mL) were incubated in the presence of  $15 \mu\text{g}$  protein/mL RLPs (RLP) or medium alone (control) for 18 hours, or pretreated with  $10 \mu\text{mol/L}$  atorvastatin (RLP+atr) for 48 hours,  $30 \mu\text{g/mL}$  C3 exoenzyme (RLP+C3) for 48 hours, or  $1 \mu\text{g/mL}$  cytochalasin D (RLP+cyto) for 10 minutes before incubation with RLPs. pFAK (397Y) and total FAK expressions were detected for each condition by Western blotting analysis ( $10 \mu\text{g}$  protein/lane). Blots are representative of 4 separate experiments. Bar graph shows the ratio of pFAK (397Y) expression to total FAK expression from 4 separate experiments.  $**P < 0.01$  vs control;  $\#P < 0.05$  vs RLPs. **B**, THP-1 cells ( $1 \times 10^6$ /mL) were transfected with FAK antisense oligonucleotides, sense oligonucleotides, or mismatched sense oligonucleotides. Total FAK expression in each condition was detected by Western blotting ( $10 \mu\text{g}$  protein/lane). Blots are representative of 3 separate experiments. Bar graph shows the ratio of total FAK expression in the membrane fraction to GAPDH expression from 3 separate experiments.  $*P < 0.05$  vs sense. **C**, THP-1 cells ( $1 \times 10^6$ /mL) transfected with FAK antisense oligonucleotides, sense oligonucleotides, or mismatched sense oligonucleotides were incubated with  $15 \mu\text{g}$  protein/mL RLPs [RLP(+)] or medium alone [RLP(-)] for 18 hours, and a static adhesion assay to HUVEC monolayers was performed. Data are from 3 separate experiments.  $*P < 0.05$  vs sense RLP(-);  $**P < 0.05$  vs mismatch sense RLP(-); and  $\#P < 0.05$  vs sense RLP(-). **D**, THP-1 cells were treated as described in **C**. Activation-dependent epitope of  $\beta_1$ -integrin (activated  $\beta_1$ -integrin) and total  $\beta_1$ -integrin expression were detected for each condition by Western blotting analysis ( $10 \mu\text{g}$  protein/lane). Blots are representative of 3 separate experiments. Bar graph shows the ratio of activation-dependent epitope expression to total  $\beta_1$ -integrin expression from 3 separate experiments.  $**P < 0.01$  vs RLP(-).

Concerning the mechanism by which RLPs activated RhoA, we showed the involvement of PKC in this process. It has been reported that RhoA is regulated by several factors.<sup>16</sup> Recently, PKC has been reported to activate RhoA by regulating guanine nucleotide dissociation inhibitor (GDI) phosphorylation in endothelial cells,<sup>17</sup> and our data indicated that RLP-induced PKC activation resulted in RhoA activation in U937 cells. This novel pathway for enhancing adhesion to vascular endothelium may be operative in U937 cells.

Remnant lipoproteins have been reported to be taken up via LDL receptor families.<sup>18</sup> In the present study, deprivation of apo E as well as the degradation of RLPs, which resulted in decreased lipid content in U937 cells, attenuated RLP-induced U937 cell adhesion. Though apo E itself failed to induce U937 cell adhesion, it may be necessary for the uptake of RLPs, as apo E not only serves as a ligand for LDL receptor families, but also interacts with cell surface LPL and heparan-sulfate proteoglycan (HSPG), facilitating cellular

lipid uptake.<sup>19</sup> These results indicate that the lipid components taken up as RLPs are responsible for their major stimulatory effects on U937 cell adhesion.

We also demonstrated that preincubation of monocytes with atorvastatin significantly decreased RLP-induced monocyte adhesion to HUVECs. As we have previously reported, the inhibitory effect of statin in monocyte adhesion involves a modulation of RhoA.<sup>6</sup> In the present study, we found that atorvastatin attenuated FAK activation as well as the expression levels of integrins induced by RLP treatment. Interestingly, CE accumulation induced by RLPs was not significantly affected by atorvastatin pretreatment (Table 2). These results indicate that atorvastatin reduces RhoA activity not by inhibiting RLP uptake, but rather by inhibiting the geranylgeranyltransferase-associated pathway.<sup>20</sup> Although we did not measure the extent of HMG-CoA reductase activity in U937 cells after atorvastatin treatment, the inhibition of HMG-CoA reductase activity by treatment with 10



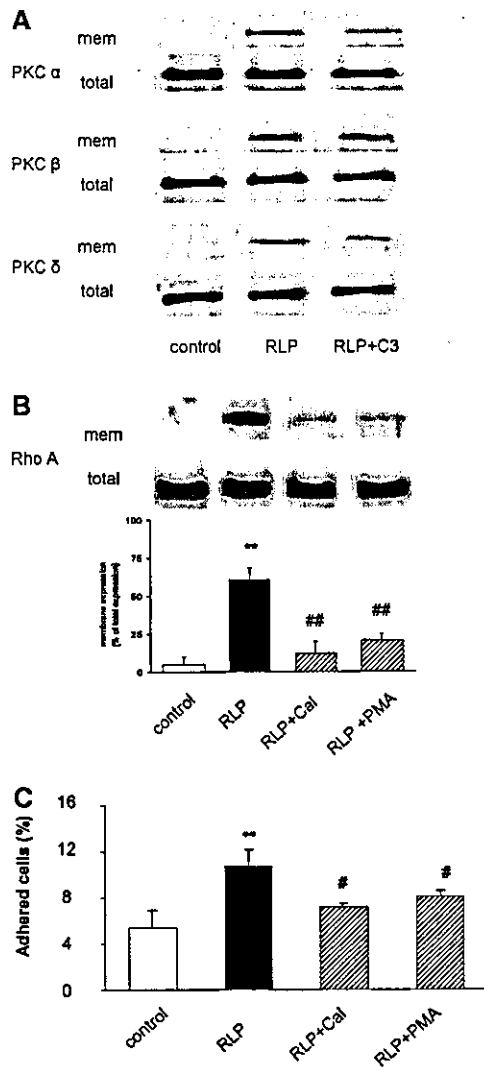


**Figure 6.** Involvement of PKC in RLP-induced RhoA activation in U937 cells. **A**, U937 cells ( $1 \times 10^6$ /mL) were incubated in the presence of  $15 \mu\text{g}$  protein/mL RLPs (RLP) or medium alone (control) for 18 hours, or pretreated with  $30 \mu\text{g}/\text{mL}$  C3 exoenzyme (RLP+C3) for 48 hours before incubation with RLPs. PKC expression was detected in the membrane (mem) and total lysate of U937 cells ( $1 \times 10^6$ /mL) for each condition by Western blotting ( $10 \mu\text{g}$  protein/lane). Blots are representative of 3 separate experiments. **B**, U937 cells ( $1 \times 10^6$ /mL) were incubated in the presence of  $15 \mu\text{g}$  protein/mL RLPs (RLP), medium alone (control) for 18 hours, or  $2.5 \mu\text{mol}/\text{L}$  calphostin C (RLP+calphostin C) for 18 hours, or pretreated with  $5 \mu\text{mol}/\text{L}$  PMA (RLP+PMA) for 18 hours before incubation with RLPs. RhoA expression was detected in the membrane (mem) and total lysate of U937 cells ( $1 \times 10^6$ /mL) for each condition by Western blotting ( $10 \mu\text{g}$  protein/lane). Blots are representative of 3 separate experiments. Bar graph shows the ratio of membrane RhoA expression to total RhoA expression from 4 separate experiments. \*\* $P < 0.01$  vs control; ## $P < 0.01$  vs RLPs. **C**, Static adhesion assay to HUVEC monolayers was performed using U937 cells ( $1 \times 10^6$ /mL) treated as described in **B**. \*\* $P < 0.01$  vs control; # $P < 0.05$  vs RLPs.

$\mu\text{mol}/\text{L}$  atorvastatin did not damage monocytic cells as described previously.<sup>21</sup> Moreover, cocubation with mevalonic acid canceled the effect of atorvastatin (Figure 2D), suggesting the importance of HMG-CoA pathway including geranylgeranyltransferase.

In summary, RLPs were found to induce the adhesion of monocytes to vascular endothelium, which may be one of the direct causative roles of remnant lipoproteins in atherogenesis. PKC activation, RhoA activation, actin polymerization, and FAK activation followed by the induction of integrin expression may also be involved in this process. Moreover, atorvastatin attenuated RLP-induced monocyte adhesion to vascular endothelium by modulating RhoA activity. From these findings, we concluded that this compound has potential clinical benefits for the treatment of patients with hypercholesterolemia as well as those with combined hyperlipidemia with elevated levels of remnant lipoproteins.

### Acknowledgments

The authors gratefully acknowledge support (10178102) and special coordination funds from the Ministry of Education, Science, Technology, and Culture of Japan. We also wish to thank the members of the Department of Obstetrics, Sanraku Hospital, Tokyo, for supplying the umbilical cords, along with Yoshie Nakamura and Naoko Tomie for their technical assistance.

### References

- Jørgen J, Hans OH, Poul S, Finn G. Triglyceride concentration and ischemic heart disease: an eight-year follow-up in the Copenhagen male study. *Circulation*. 1998;97:1029–1036.
- Phillips NR, Waters D, Havel RJ. Plasma lipoproteins and progression of coronary artery disease evaluated by angiography and clinical events. *Circulation*. 1993;88:2762–2770.
- Kawakami A, Tanaka A, Nakano T, Saniabadi A, Numano F. Stimulation of arterial smooth muscle cell proliferation by remnant lipoprotein particles isolated by immuno-affinity chromatography with anti-apo A-I and anti-apo B-100. *Horm Metab Res*. 2001;33:67–72.
- Ross R. Atherosclerosis: an inflammatory disease. *N Engl J Med*. 1999;340:115–126.
- Doi H, Kugiyama K, Oka H, Sugiyama S, Ogata N, Koide S, Nakamura S, Yasue H. Remnant lipoproteins induce proatherothrombotic molecules in endothelial cells through a redox-sensitive mechanism. *Circulation*. 2000;102:670–676.
- Yoshida M, Sawada T, Ishii H, Gerszten RE, Rosenzweig A, Gimbrone M Jr, Yasukochi Y, Numano F. HMG-CoA reductase inhibitor modulates monocyte-endothelial cell interaction under physiological flow conditions in vitro involvement of Rho GTPase-dependent mechanism. *Arterioscler Thromb Vasc Biol*. 2001;21:1165–1171.
- Nakajima K, Saito T, Tamura A, Suzuki T, Nakano T, Adachi M, Tanaka A, Tada N. A new assay method for the quantification of cholesterol in remnant like lipoproteins in human serum using monoclonal anti apo B-100 and apo A-I immunoaffinity mixed gels. *Clin Chim Acta*. 1993;223:53–71.
- Lowry DH, Rosenbrough NJ, Farr AL, Randall RJ. Protein measurement with the folin phenol reagent. *J Biol Chem*. 1951;193:165–175.
- Kohno H, Sueshige N, Oguri K, Izumidate H, Masunari T, Kawamura M, Itabe H, Takano T, Hasegawa A, Nagai R. Simple and practical sandwich-type enzyme immunoassay for human oxidatively modified low density lipoprotein using antioxidantized phosphatidylcholine monoclonal antibody and antihuman apolipoprotein-B antibody. *Clin Biochem*. 2000;33:243–253.
- Bradley WA, Hwang SL, Karlin JB, Lin AH, Prasad SC, Gotto AM Jr, Gianturco SH. Low-density lipoprotein receptor binding determinants switch from apolipoprotein E to apolipoprotein B during conversion of hypertriglyceridemic very-low-density lipoprotein to low-density lipoproteins. *J Biol Chem*. 1984;259:14728–14735.
- Luscinskas FW, Brock AF, Amaout MA, Gimbrone M Jr. Endothelial-leukocyte adhesion molecule-1-dependent and leukocyte (CD11/CD18)-dependent mechanisms contribute to polymorphonuclear leukocyte adhesion to cytokine-activated human vascular endothelium. *J Immunol*. 1989;142:2257–2263.
- Hatton JP, Gaubert F, Lewis ML, Darsel Y, Ohlmann P, Cazenave JP, Schmitt D. The kinetics of translocation and cellular quantity of protein

- kinase C in human leukocytes are modified during spaceflight. *FASEB J*. 1999;13 suppl:S23-S33.
12. Schneeman BO, Kotite L, Todd KM, Havel RJ. Relationships between the responses of triglyceride-rich lipoproteins in blood plasma containing apolipoproteins B-48 and B-100 to a fat-containing meal in normo-lipidemic humans. *Proc Natl Acad Sci U S A*. 1993;90:2069-2073.
  13. Wojciak-Stothard B, Williams L, Ridley AJ. Monocyte adhesion and spreading on human endothelial cells is dependent on Rho-regulated receptor clustering. *J Cell Biol*. 1999;145:1293-1307.
  14. Zachary I, Rozengurt E. Focal Adhesion Kinase (p125FAK): a point of convergence in the action of neuropeptides, integrins, and oncogenes. *Cell*. 1992;71:891-894.
  15. Schaller MD, Hildebrand JD, Shannon JD, Fox JW, Vines RR, Parsons JT. Autophosphorylation of the focal adhesion kinase, pp125FAK, directs SH2- dependent binding of pp60src. *Mol Cell Biol*. 1994;14:1680-1688.
  16. Kranenburg O, Moolenaar WH. Ras-MAP kinase signaling by lysophosphatidic acid and other G protein-coupled receptor agonists. *Oncogene*. 2001;26:1540-1546.
  17. Mehta D, Rahman A, Malik AB. Protein kinase C- $\alpha$  Signals Rho-guanine nucleotide dissociation inhibitor phosphorylation and Rho activation and regulates the endothelial cell barrier function. *J Biol Chem*. 2001;276:22614-22620.
  18. Argmann CA, Van Den Diepstraten CH, Sawyez CG, Edwards JY, Hegele RA, Wolfe BM, Huff MW. Transforming growth factor- $\beta$ 1 inhibits macrophage cholesteryl ester accumulation induced by native and oxidized VLDL remnants. *Arterioscler Thromb Vasc Biol*. 2001;21:2011-2018.
  19. Huff MW, Miller DB, Wolfe BM, Connelly PW, Sawyez CG. Uptake of hypertriglyceridemic very low density lipoproteins and their remnants by HepG2 cells: the role of lipoprotein lipase, hepatic triglyceride lipase, and cell surface proteoglycans. *J Lipid Res*. 1997;38:1318-1333.
  20. Liu L, Moesner P, Kovach NL, Baily R, Hamilton AD, Sebti SM, Harlan JM. Integrin-dependent leukocyte adhesion involves geranylgeranylated protein(s). *J Biol Chem*. 1999;274:33334-33340.
  21. Grip O, Janciauskiene S, Lindgren S. Atorvastatin activates PPAR- $\gamma$  and attenuates the inflammatory response in human monocytes. *Inflamm Res*. 2002;51:58-62.

## Hypoxia-Induced Upregulation of CD11b Expression in Granulocytes

Masatoshi Jibiki, M.D., F.I.C.A., Masayuki Yoshida, M.D., Yoshinori Inoue, M.D., Lee Jung Chien, M.D., Takehisa Iwai, M.D., F.I.C.A., Yukio Yasukochi, M.D.

Departments of Surgery and Applied Genetics, Graduate School of Medicine, Tokyo Medical and Dental University, Tokyo, Japan

**Abstract.** The aim of this study is to evaluate leukocyte-endothelial adhesion during ischemia/reperfusion injury. Polymorphonuclear neutrophils (PMN) were isolated from healthy volunteers and incubated in the presence of 2% O<sub>2</sub> (hypoxia) or 21% O<sub>2</sub> (normoxia) at 37°C for two hours. In some experiments, whole blood was subjected to hypoxia or normoxia prior to PMN isolation. Flowcytometric analysis and adhesion assays were carried out using these PMN. Moreover, adhesion assay was carried out using PMN, prepared from the patients who underwent infrarenal aortic aneurysmectomy with aortic clamping at various time points as an in vivo model of ischemial reperfusion injury. Flowcytometric analysis revealed an increased expression of CD11b in PMN subjected to hypoxia compared with those subjected to normoxia prior to isolation. Interestingly, these phenomena were not observed with PMN isolated prior to being subjected with hypoxia. Enzyme-linked immunosorbent assay (ELISA) using serum prepared from whole blood subjected to hypoxia revealed elevated levels of tumor necrosis factor (TNF)- $\alpha$  compared with those subjected to normoxia. PMN obtained during aneurysmectomy exhibited an increased adhesion to activated human umbilical vein endothelial cells (HUVEC), compared with those taken from the same patients prior to the operation. In contrast, PMN prepared after aortic clamp, exhibited a significant reduced adhesion to activated HUVEC. Hypoxic condition, induced CD11b expression on PMN in vitro. PMN subjected to hypoxic condition in vivo exhibited an increased adhesion to activated endothelium. Elevated level of serum TNF- $\alpha$  may be involved in this phenomenon.

### Introduction

Ischemia/reperfusion (I/R) injury has been one of the most serious problems after vascular reconstruction in chronic critical limb ischemia or acute arterial ischemia. Numerous studies suggested that leukocyte-endothelial interactions played an important role in pathogenesis of these conditions. The release of mediators due to hypoxia may result in the expression of surface adhesion molecules on endothelial cells [1,2] as well as polymorphonuclear neutrophils (PMN) [1,3,4]. It has recently been shown that hypoxia increases the adherence of granulocytes to endothelial cells through an increased production of platelet-activating factor (PAF) by hypoxic endothelial cells [1]. Korthuis et al. [5] have achieved leukocyte depletion using leukocyte filter, as the result, prevented the increases in vascular permeability and vascular resistance. Crinnion et al. [6] have reported that neutrophil recruitment and muscle infarction are reduced using anti-MAC 1 monoclonal antibody. Monoclonal antibodies (mAb) to CD11b appear to have a beneficial effect in canine myocardial injury [7]. So far, the importance of PMN-endothelial interaction has been emphasized in I/R injury [8,9], but no direct evidence has been provided whether hypoxia directly affects PMN function or not.

The aim of this study is to assess the possible effects of hypoxia on I/R and we also extended our research utilizing a sample obtained from patients who underwent an elective aneurysmectomy to investigate in vivo effect of PMN adhesion to vascular endothelial cells after I/R.

### Materials and Methods

#### Reagents

RPMI-1640, Dulbecco's phosphate buffered saline (DPBS) and Hank's balanced salt solution (HBSS) were obtained from Sigma. Fetal bovine

---

Correspondence to: Masatoshi Jibiki, M.D., F.I.C.A., Department of Surgery, Graduate School of Medicine, Tokyo Medical and Dental University, 1-5-45 Yushima, Bunkyo-ku, Tokyo, 113-8519, Japan

serum (FBS) was purchased from GIBCO BRL (Grand Island, NY). Paraformaldehyde was purchased from Fischer Scientific (Springfield, NJ). Recombinant human interleukin (IL)-1  $\beta$  was obtained from Biogen (Cambridge, MA). Biscarboxyethyl-carboxyfluorescein acetoxymethyl ester (BCECF) was purchased from Molecular Probes (Eugene, OR). mAb to CD11a, CD11b, CD18, and sialyl Lewis<sup>x</sup> (sLX) were obtained from Pharmingen (San Diego, CA), mAb to L-selectin was obtained from Serotec (Oxford, England). Human umbilical vein endothelial cells (HUVEC) were isolated and established in culture, as previously described by Yoshida M et al. [10]. Primary cultures were serially passaged ( $\leq$  1:3 split ratio) and maintained in Medium 199 buffered with 25 mmol/L HEPES and supplemented with 10% FBS, endothelial cell growth factor (25  $\mu$ g/ml), and porcine intestinal heparin (50  $\mu$ g/ml). For experimental use, subcultured (passage 2 or 3) endothelial cells were plated on gelatin-coated 35-mm tissue culture dishes.

### PMN Preparation

PMN were isolated from citrated blood drawn from normal volunteers using dextran sedimentation followed by Ficoll-hypaque centrifugation. Hypotonic lysis was used to remove erythrocytes. Then, PMN ( $1 \times 10^6$ /ml) were subjected to a hypoxic condition (2% O<sub>2</sub>) (hypoxia) or a normoxic condition (21% O<sub>2</sub>) (normoxia) for 2 hours at 37°C. In some experiments, whole blood was directly subjected to a hypoxic condition or a normoxic condition for two hours at 37°C, then PMN were isolated as described above.

### Flowcytometric Analysis

PMN were prepared for flowcytometry using previously described methods [11]. Briefly, PMN ( $0.5 \times 10^6$  per condition) were washed with RPMI-1640 contained +1% FBS, and incubated in the presence of indicated mAb for 45 minutes. After three washings with RPMI + 1% FBS, fluorescein isothiocyanate (FITC)-goat anti-mouse polyclonal immunoglobulin (Ig) G was added at 1:200 dilution ratio and incubated for 45 minutes. After an additional three washings, the PMN were fixed with 3% paraformaldehyde and surface expression of adhesion molecules in PMN was measured by a fluorescence activated cell sorter (FACS) caliber (Becton-Dickinson). A total of 10,000 cells were analyzed for each measurement.

### Adhesion Assay

A human leukocyte cell line, HL-60 cells, prelabeled with the fluorescent dye BCECF were added ( $1.6 \times 10^6$  cells/well in RPMI + 1% FBS) to monolayers of HUVEC in 35-mm dishes. After incubation under static adhesion assay conditions, nonadherent HL-60 cells were removed by washing three times with RPMI + 1% FBS, and the monolayer-associated HL-60 cells were collected into HBSS + 5 mM ethylenediaminetetraacetic acid (EDTA) and their fluorescence measured in a fluorescent plate reader (Perceptive Biosystems), as previously described (Yoshida M, 1996) [10].

### Tumor Necrosis Factor (TNF)- $\alpha$ Measurement

Whole blood drawn from healthy normal volunteers in the presence of anti-coagulant were subjected to a hypoxic condition (2% O<sub>2</sub>) or a normoxic condition (21% O<sub>2</sub>) for two hours at 37°C. Plasma fraction was collected after centrifugation at 2,500 r.p.m. for 15 minutes. TNF- $\alpha$  in plasma was measured using the human TNF- $\alpha$  ultrasensitive Enzyme-Linked Immunosorbent Assay (ELISA) (COSMO-BIO, Tokyo, Japan).

### PMN Preparation During Vascular Surgery Operation

Blood samples were collected from the patients who underwent an elective aneurysmectomy and a bifurcated graft replacement for infrarenal abdominal aortic aneurysm (n = 5) as described in Table 1 after obtaining informed consent. The abdominal aorta and bilateral external iliac arteries (EIA) were clamped while the proximal and distal anastomosis were accomplished. Blood samples were taken from the left femoral vein at four different time points, 1. prior to the aortic clamping (control), 2. just before the aortic declamp, 3. 5 minutes after the aortic declamp, 4. 20 minutes after the aortic declamp. PMN were isolated from each blood sample as described above and adhesion assay was carried out under static condition.

### Results

First, we examined whether hypoxia modulated surface expression of adhesion molecules on PMN. PMN were isolated from whole blood, drawn from healthy volunteers in the presence of anti-coagulant, then were subjected to a hypoxic condition or a normoxic condition for two hours at 37°C (PMN hypoxia). Flowcytometric analysis revealed that no significant changes were observed for CD11a, CD11b, CD18 expression between those subjected to hypoxia (black line) and normoxia (gray area) (Figure 1, PMN hypoxia). In contrast, when PMN were subjected to hypoxia prior to isolation from whole blood, expression of CD11b was significantly increased (Figure 1, whole blood hypoxia). The expression levels of other adhesion molecules (CD11a and CD18) were not changed under these assay conditions.

To evaluate adhesion capabilities of these PMN subjected to hypoxia prior to isolation from whole blood, adhesion assay was conducted under static condition. As shown in Figure 2, the number of adherent PMN to HUVEC activated with IL-1 $\beta$  for four hours were not significantly changed between those subjected to pre-isolation hypoxia and normoxia. Adhesion assay utilizing PMN subjected to post-isolation hypoxia also

Table 1. Blood samples were collected from the patients who underwent an elective aortic aneurysmectomy and a bifurcated graft replacement for infrarenal abdominal aortic aneurysm (n = 5) after obtaining informed consent

Patient	Gender	Age (y.o.)	Diagnosis	Comorbidity
1.	Male	75	I.R. AAA	none
2.	Male	63	I.R. AAA	none
3.	Male	71	I.R. AAA	LC, DM
4.	Male	73	I.R. AAA, rt. IIAA	post gastrectomy
5.	Male	75	I.R. AAA	HT

I.R. AAA: infrarenal abdominal aortic aneurysm, IIAA: internal iliac artery aneurysm, LC: liver cirrhosis, HT: hypertension, DM: diabetes mellitus.

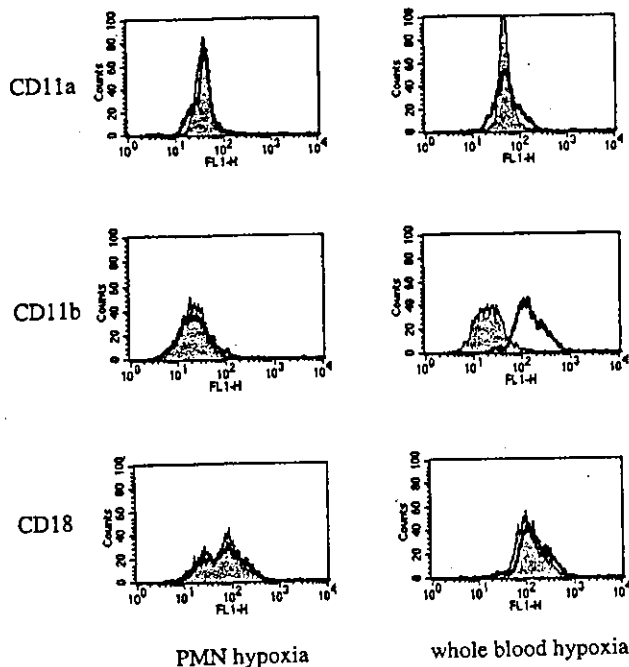


Fig. 1. Polymorphonuclear neutrophils (PMN) were isolated from whole blood of healthy volunteers in the presence of anti-coagulant, then were subjected to a hypoxic condition (2% O<sub>2</sub>) or a normoxic condition (21% O<sub>2</sub>) for two hours at 37°C (PMN hypoxia). The flowcytometric analysis revealed that no significant changes were observed for CD11a, CD11b, CD18 expression between those subjected to hypoxia (black line) and normoxia (gray area). In contrast, when PMN were subjected to hypoxia prior to isolation from whole blood, expression of CD11b was significantly increased (whole blood hypoxia).

exhibited similar level of adhesion to those subjected to normoxia (data not shown).

To analyze soluble factor which potentially mediates CD11b upregulation in PMN subjected to pre-isolation hypoxia, we measured the serum TNF- $\alpha$  level obtained from the whole blood subjected to hypoxic condition for two hours. As shown in Figure 3, serum subjected to hypoxia exhibited significantly higher level of TNF- $\alpha$  ( $8.40 \pm 1.09$  pg/ml) than that exposed to normoxic condition ( $3.88 \pm 0.62$  pg/ml) ( $p < 0.05$ ).

To further investigate the effect of hypoxia on PMN function *in vivo*, PMN were prepared from blood sample obtained during an elective bifurcated graft replacement for infrarenal abdominal aortic aneurysm. In this operation, the bilateral EIAs of the patients were clamped during a graft replacement, blood flow was restored to the EIA for the lower extremity. Basic profiles and characteristics of patients were described in Table 1. The average duration for left EIA clamping was  $90.8 \pm 17.7$  minutes (5 cases). Blood samples were collected from the left femoral vein at 4 different time points (prior to the aortic clamping (control), just before, 5 minutes, 20 minutes after the aortic clamping was released). As shown Figure 4, the percent adhesion of PMN isolated during the aortic clamping to the activated HUVEC was significantly increased compared to PMN isolated prior to the aortic clamping (control). Interestingly, the percent adhesion of PMN isolated after the declamping was lower than that of aortic clamping.

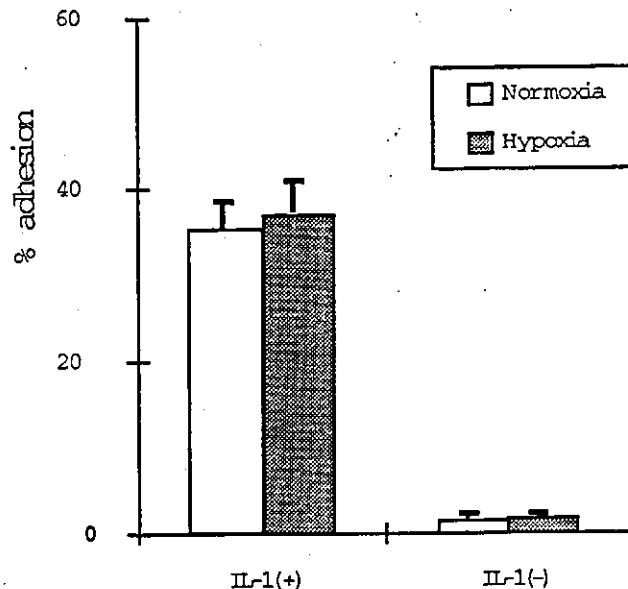


Fig. 2. Adhesion assay of hypoxic polymorphonuclear neutrophils (PMN) with cytokine was activated. The number of adherent PMN to human umbilical vein endothelial cells (HUVEC) activated with interleukin (IL)-1 $\beta$  for four hours was investigated using PMN subjected to hypoxia or normoxia for two hours.

## Discussion

I/R injury has been one of the major complications during and after vascular surgery. Previous studies reported the elevated surface expression of adhesion molecules in PMN including CD11b and CD18 [5]. However, the mechanisms underlying the effect of hypoxia in upregulation of adhesion molecules were not fully examined. In this paper, we studied whether PMN, when subjected to hypoxic condition, overexpressed functional adhesion molecules which could participate in PMN-endothelial interaction. As we demonstrated, PMN subjected to hypoxia after their isolation from whole blood failed to exhibit enhanced expression of CD11b. In contrast, when PMN were subjected to hypoxia prior to isolation, a significant upregulation of CD11b was observed. However, adhesion to activated HUVEC of these PMN subjected to hypoxia prior to isolation was not dramatically changed compared with the control PMN. Therefore, there should be still unknown mechanism(s) that contributed to determine adhesion capability of hypoxic PMN in addition to expression level of CD11b. It was also conceivable that adhesive interaction between PMN and endothelial cells might not be a primal event during I/R injury. Other factors from PMN (cytokines, chemokines) could potentially play critical roles under these conditions. It has recently been shown that hypoxia increases the adhesion of granulocytes to endothelium by inducing PAF production from endothelium [1]. Thus, the requirement of whole blood to induce CD11b expression in PMN during hypoxia suggests the existence of soluble factors in the plasma exposed to hypoxia that mediates integrin upregulation. One of the candidate substances is TNF- $\alpha$ , Barry et al. [18] reported that monocyte was the source

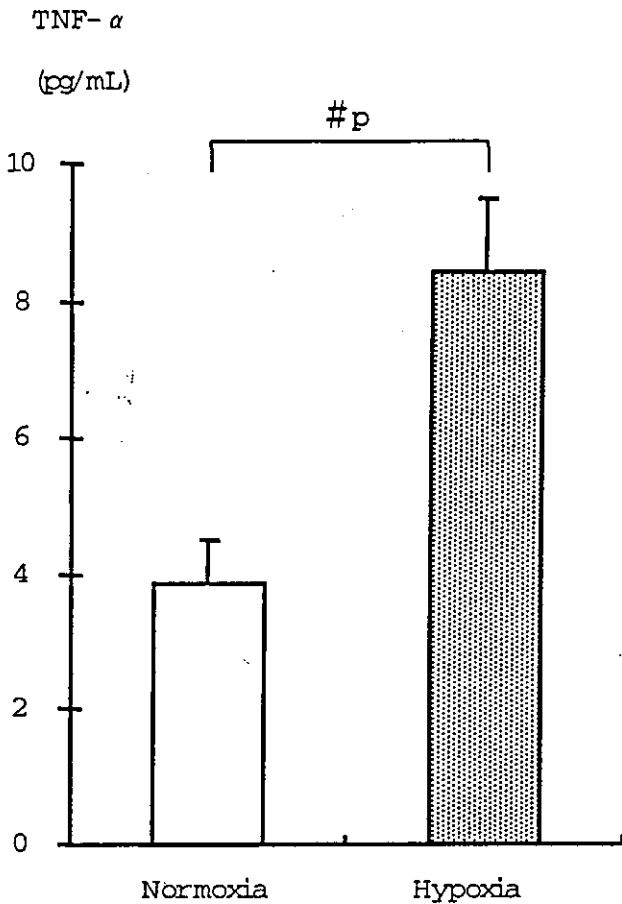


Fig. 3. The serum from the whole blood subjected to hypoxia exhibited significantly higher level of tumor necrosis factor (TNF)- $\alpha$  than that exposed to normoxic condition. #*p* < 0.05 vs. normoxia.

of TNF- $\alpha$  in the early stages of reperfusion from their studies. It has been shown that serum level of cytokines (TNF- $\alpha$ , IL-1, IL-6) was increased during the reperfusion process following hind limb ischemia in anesthetized rat [13]. Moreover, an acute hindlimb ischemia and reperfusion initiates a systemic TNF response during the ischemic period that is partly responsible for the associated skeletal muscle injury [14]. In fact, in our experiments, the concentration of TNF- $\alpha$  in the serum exposed to hypoxia was significantly higher than normoxia-exposed serum. Although precise mechanism(s) remains unclear, increased level of serum TNF- $\alpha$  may be associated with CD11b upregulation after hypoxia, and may be implicated as early initiators of this response to visceral ischemic-reperfusion injury [14]. A role for TNF- $\alpha$  in I/R injury has been also confirmed by protective effects of anti-TNF antibodies in hepatic, intestinal and limb ischemia [15-17].

Based on these *in vitro* findings, we then decided to seek the *in vivo* effect of hypoxia to PMN endothelial adhesion, using samples collected from the patients undergoing operations for abdominal aortic aneurysm. Previously, Barry et al. [18] reported that leukocytes were activated by artery-clamp with CD11b upregulation. However actual adhesion characteristics of these leukocytes remained unclear. Our results of adhesion assay using PMN prepared from patients with vascular surgery provided important biological evidence for PMN-endothelial interaction during I/R injury. Maximum increase of PMN adhesion was observed when PMN collected in the middle of aortic clamp (hypoxic condition) in our study. This made an interesting contrast to the data from Barry et al. [18] showing that maximum increase of CD11b expression was detected 5 minutes after the release of aortic clamp (reperfusion period). One of the reasons for this discrepancy could be

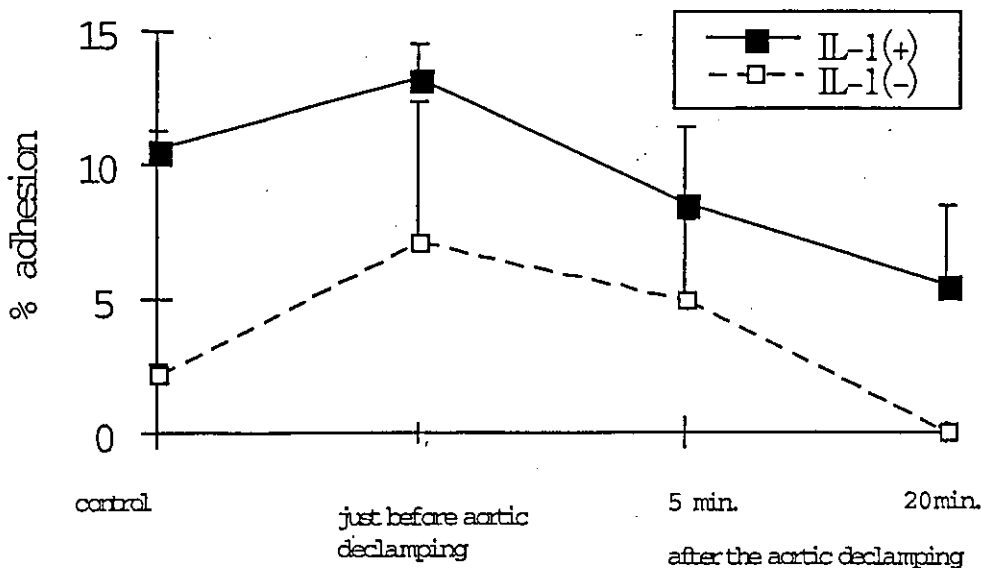


Fig. 4. The adhesion of polymorphonuclear neutrophils (PMN) isolated during the operation using aortic clamp procedure to cultured endothelium: PMN were isolated at different time points during the operation, and adhesion assay using activated human umbilical vein endothelial cells (HUVEC) were carried out. The percent adhesion increased significantly in the aortic clamping period than the control (prior to the aortic clamping). Interestingly, the percent adhesion of PMN isolated after declamping was lower than that of aortic clamping.

the difference of vascular beds that PMN were prepared from. We drew blood from the left femoral vein, proximate to ischemic artery, whereas Barry et al. collected blood samples from the inferior vena cava. The results of our experiments demonstrate the importance of the PMN and soluble factors on I/R injury.

In conclusion, we have identified that hypoxia increased CD11b expression but not CD11a or CD18 of PMN. This enhanced expression of CD11b may involve elevated level of serum TMN- $\alpha$  during hypoxic condition. These findings may have important implications to understanding the mechanism of I/R injury.

## References

- Milhoan KA, Lane TA, Bloor CM (1992) Hypoxia induces endothelial cells to increase their adherence for neutrophils: role of PAF. *Am J Physiol* 263:H956-962.
- Ascer E, Gennaro M, Cupo S, Mohan C (1992) Do cytokines play a role in skeletal muscle ischemia and reperfusion? *J Cardiovasc Surg* 33:588-592.
- Arnould T, Michiels C, Remacle J (1993) Increased PMN adherence on endothelial cells after hypoxia: involvement of PAF, CD18/CD11b and ICAM-1. *Am J Physiol* 264:C1102-1110.
- Palluy O, Morliere L, Gris JC, Bonne C, Modat G (1992) Hypoxia/reoxygenation stimulates endothelium to promote neutrophil adhesion. *Free Radic Biol Med* 13:21-30.
- Korthuis RJ, Grisham MB, Granger DN (1988) Leukocyte depletion attenuates vascular injury in postischemic skeletal muscle. *Am J Physiol* 254:H823-827.
- Crinnion JN, Homer-Vanniasinkan S, Parkin SM, Gough MJ (1996) Role of neutrophil-endothelial adhesion in skeletal muscle reperfusion injury. *Br J Surg* 83:251-254.
- Simpson PJ, Todd FR, Fantone JC, Michelson JK, Griffin JD, Lucchesi BR (1988) Reduction of experimental myocardial reperfusion injury by a monoclonal antibody (Anti-Mol, Anti-CD11b) that inhibits leukocyte adhesion. *J Clin Invest* 81:624-629.
- Arnould T, Michiels C, Janssens D, Delaive E, Remacle J (1995) Hypoxia induces PMN adherence to umbilical vein endothelium. *Cardiovasc Res* 30:1009-1016.
- Franciose RJ, Moore EE, Moore FA, Read A, Carl VS, Banerjee A (1996) Hypoxia/reoxygenation of human endothelium activates PMNs to detach endothelial cells via a PAF mechanism. *J Surg Res* 61:459-462.
- Yoshida M, Westlin WF, Wang N, Ingber DE, Rosenzweig A, Resnick N, Gimbrone Jr MA (1996) Leukocyte adhesion to vascular endothelium induces E-selectin linkage to the actin cytoskeleton. *J Cell Biol* 133:445-455.
- Wallace PJ, Wersto RP, Pakman CH, Lichtman MA (1984) Chemotactic peptide-induced changes in neutrophil actin conformation. *J Cell Biol* 99:1060-1065.
- Scannell G, Waxman K, Vaziri ND, Zhang J, Kaupke CJ, Jalali M, Hect C (1995) Effects of trauma on leukocyte intercellular adhesion molecule-1, CD11b, and CD18 expressions. *J Trauma* 39:641-644.
- Seekamp A, Warren JS, Remick DG, Till GO, Ward PA (1993) Requirements for TNF- $\alpha$  and IL-1 in limb ischemia reperfusion injury and associated lung injury. *Am J Pathol* 143:453-463.
- Gaines GC, Welborn MB III, Moldawre LL, Huber TS, Seeger JM (1999) Attenuation of skeletal muscle ischemia/reperfusion injury by inhibition of tumor necrosis factor. *J Vasc Surg* 29:370-376.
- Caty MG, Guice KS, Oldam KT, Remick DG, Kunkel SI (1990) Evidence for tumor necrosis factor-induced pulmonary microvascular injury after intestinal ischemia-reperfusion injury. *Ann Surg* 21:694-700.
- McMillen MA, Huribal M, Sumpio B (1993) Common pathway of endothelial-leukocyte interaction in shock, ischemia, and reperfusion. *Am J Surg* 166:557-562.
- Pober JS, Slowick MR, De Luca LG, Ritchie AJ (1993) Elevated cyclic AMP inhibits endothelial cell synthesis and expression of TNF-induced endothelial leukocyte adhesion molecule-1, and vascular adhesion molecule-1, but not intercellular adhesion molecule-1. *J Immunol* 150:5114-5123.
- Barry MC, Kelly C, Burke P, Sheehan S, Redmond HP, Bouchier-Hayes D (1997) Immunological and physiological responses to aortic surgery; effect of reperfusion on neutrophil and monocyte activation and pulmonary function. *Br J Surg* 84:513-519.

# E-Selectin Polymorphism Associated With Myocardial Infarction Causes Enhanced Leukocyte-Endothelial Interactions Under Flow Conditions

Masayuki Yoshida, Yoshio Takano, Taishi Sasaoka, Toru Izumi, Akinori Kimura

**Objective**—Polymorphisms found in genes encoding adhesion molecules have been reported to be associated with atherosclerosis. We investigated the Ser128Arg polymorphism in the E-selectin gene in Japanese patients with myocardial infarction and its functional significance.

**Methods and Results**—Results from 135 patients with myocardial infarction and 327 control subjects revealed that the frequency of Arg128-positive was significantly higher in the patients than in controls (12.6% versus 6.7%; odds ratio, 2.0; 95% CI, 1.04 to 3.85), indicating that the Ser128Arg polymorphism was associated with myocardial infarction. We then generated a recombinant E-selectin adenovirus carrying a mutation (AdS128R-E) and compared it with its wild-type counterpart by evaluating the adhesion characteristics of transduced human umbilical vein endothelial cells under flow. AdS128R-E-transduced human umbilical vein endothelial cells supported significantly more rolling and adhesion of neutrophils and mononuclear cells compared with human umbilical vein endothelial cells transduced with AdWT-E ( $P < 0.001$ ) and also exhibited significantly greater levels of phosphorylation of extracellular signal regulated kinase 1 and 2 and p38 mitogen-activated protein kinase, suggesting that an altered endothelial signaling pathway is associated with this polymorphism.

**Conclusions**—Our results suggest that the E-selectin Ser128Arg polymorphism can functionally alter leukocyte-endothelial interactions as well as biochemical and biological consequences, which may account for the pathogenesis of myocardial infarction. (*Arterioscler Thromb Vasc Biol.* 2003;23:783-788.)

**Key Words:** E-selectin ■ polymorphism ■ endothelium ■ leukocyte adhesion ■ mitogen-activated protein kinase

Leukocyte-endothelial interactions contribute to a variety of vascular disease processes, such as acute and chronic inflammation and atherosclerosis.<sup>1</sup> Several soluble factors (eg, cytokines, chemokines, and growth factors), as well as cell surface adhesion molecules, which are expressed by both endothelial cells and leukocytes, interact in a complex fashion to efficiently mediate leukocyte recruitment.<sup>2</sup> The selectin family of adhesion molecules shares a unique mosaic structure consisting of an amino-terminal lectin-like domain followed by an epidermal growth factor (EGF)-like domain, a variable number of complement regulatory repeats, a transmembrane domain, and a short cytoplasmic domain.<sup>3</sup> E-selectin, one of the three members of this family, has been shown to support the rolling of leukocytes on activated endothelial cells<sup>3</sup> and may also participate in the transition to stable adhesion that precedes transmigration.<sup>4</sup>

Several recent findings regarding the genetic background of atherosclerosis have indicated that DNA polymorphisms in genes encoding adhesion molecules are associated with a higher risk of severe atherosclerosis.<sup>5,6</sup> Moreover, it was

recently shown in a German population that a serine to arginine exchange at the 128th amino acid in the EGF domain of the E-selectin gene has a possible association with severe atherosclerosis.<sup>5,7</sup> Using a recombinant chimeric protein-based analysis,<sup>8</sup> this mutation was reported to change the binding specificity of E-selectin; however, the physiological importance of this polymorphism in the pathogenesis of vascular diseases is not yet fully understood. Because E-selectin has a role in inflammation and atherosclerosis, we attempted to analyze the association of this mutation with myocardial infarction in Japanese patients as well as elucidate its functional consequences under more physiological conditions.

## Methods

### Cell Culture and Reagents

Human umbilical vein endothelial cells (HUVECs) were isolated from normal-term umbilical veins and then cultured in 0.1% gelatin-coated tissue culture dishes in RPMI-1640 with 20% FCS (Life Technologies Oriental Inc), as described previously.<sup>9</sup> HL60 cells

Received January 27, 2003; revision accepted March 3, 2003.

From the Department of Vascular Medicine and Medical Biochemistry (M.Y., Y.T.), Graduate School of Medicine, Tokyo Medical and Dental University; Department of Cardiology (T.S., T.I.), Kitasato University School of Medicine; and Department of Molecular Pathogenesis (A.K.), Medical Research Institute, Tokyo Medical and Dental University, Tokyo, Japan.

Correspondence to Masayuki Yoshida, MD, Department of Vascular Medicine and Medical Biochemistry, Graduate School of Medicine, Tokyo Medical and Dental University, 1-5-45, Yushima Bldg D-256, Bunkyo-ku, Tokyo 113-8519, Japan. E-mail masa.vasc@tmd.ac.jp

© 2003 American Heart Association, Inc.

*Arterioscler Thromb Vasc Biol.* is available at <http://www.atvbaha.org>

DOI: 10.1161/01.ATV.0000067427.40133.59



were obtained from the American Type Culture Collection (Rockville, Md) and cultured in RPMI-1640 containing 10% FCS. Polymorphonuclear neutrophils (PMNs) and peripheral blood mononuclear cells (PBMNCs) were isolated from whole blood drawn from healthy volunteers, as described previously.<sup>10</sup> For use in a flow chamber apparatus, HUVECs (passages 2 and 3) were plated on 22-mm fibronectin-coated glass coverslips, as previously described.<sup>11</sup> Anti-extracellular signal regulated kinase (ERK) 1/2, anti-phospho-ERK1/2 (Thr202/Tyr204), and anti-p38 mitogen-activated protein kinase (MAPK) kinase were obtained from New England Biolabs (Beverly, Mass), whereas anti-phospho-p38 MAPK (Tyr180/182) antibodies were purchased from Biosource International (Camarillo, Calif).

### Genetic Analysis

The study population was comprised of 135 unrelated Japanese individuals (103 male and 32 female) who had been admitted to Kitasato University Hospital with a diagnosis of myocardial infarction (MI) and given their informed consent to the study. The mean age of onset in all patients was  $57.7 \pm 8.1$  years. The diagnosis of MI was based on typical ECG changes as well as increased serum levels of creatinine kinase and lactate dehydrogenase and was confirmed by the presence of wall motion abnormalities or responsive stenosis in any of the coronary arteries, as documented by coronary angiography. Three hundred twenty-seven subjects (229 male and 98 female, mean age  $47.6 \pm 7.9$  years) with normal ECG results and no clinical signs of coronary artery disease were also used as control subjects. A blood sample was collected from all patients and control subjects, and genomic DNA was isolated with a DNA extraction kit (Promega), according to the manufacturer's protocol. Exon 3 of the E-selectin gene was amplified by polymerase chain reaction (PCR) using the following primer pair: F1, 5'-AGT AAT AGT CCT CCT CAT CAT G-3' and R1, 5'-ACC ATC TCA AGT GAA GAA AGA G-3'. The PCR products were analyzed for the restriction-fragment length polymorphism using PstI, as described previously.<sup>6</sup>

### Construction and Expression of Recombinant E-Selectin Adenovirus

The wild-type (WT) E-selectin adenovirus (AdWT-E) and a control adenovirus carrying a nuclear-targeted form of  $\beta$ -galactosidase (AdRSV $\beta$ LacZ) have been previously described in detail.<sup>9</sup> pAdRSV4 plasmid vectors containing the entire E-selectin coding region (pAdRSVE-sel) were used to generate a point mutation from A to C at the 561st nucleotide using a Quick Change Mutagenesis kit (Stratagene) with the following complement oligonucleotides: 5'-CAA TAC ATC CTG CCG TGG CCA CGG T-3' and 5'-ACC GTG GCC ACG GCA GGA TGT ATT G-3'. The resulting shuttle vector (pAdRSVS128R-E) expressed an E-selectin protein that contained arginine, an amino acid, instead of serine at the 128th position. The recombinant adenovirus (AdS128R-E) was produced using pAdRSVS128R-E and pJM17, as described previously.<sup>9</sup> Therefore, both AdWT-E and AdS128R-E were under the control of identical regulatory elements. Viral titers of purified stocks were determined by plaque assays for 293 cells, as previously described,<sup>10</sup> and several different viral stocks were used in the present study. Stock titers ranged from  $10^9$  to  $10^{10}$  pfu/mL, with particle-to-pfu ratios of approximately  $10^2$ . E-selectin expression on the surface of HUVECs was examined 72 hours after transduction into HUVECs using a fluorescent immunoassay, as previously described,<sup>9</sup> with anti-E-selectin mAbs (7A9<sup>12</sup> and H4/18<sup>13</sup>). In brief, HUVEC monolayers were incubated on ice with either 7A9 or H4/18 at a concentration of 10  $\mu$ g/mL in RPMI-1640+1% FBS for 45 minutes. Plates were washed 3 times with RPMI-1640+1% FBS and then incubated with FITC-conjugated goat anti-murine polyclonal IgG F(ab')<sub>2</sub> (purchased from Amersham Pharmacia Biotech, Clearbrook, Ill) diluted 1:50 in Dulbecco's PBS (DPBS) containing 0.9 mmol/L CaCl<sub>2</sub> and 0.33 mmol/L MgCl<sub>2</sub> on ice for 45 minutes. The plates were then washed twice with DPBS+20% FBS and twice with DPBS alone. Cells were lysed with 0.15 mL of 0.01% NaOH in 0.1% SDS to

detect cell-surface-associated fluorescent intensity using a fluorescent plate reader (Cytofluor II, Perseptive Biosystems).

### Adhesion Assay Under Laminar Flow

The parallel-plate flow chamber used in the present study has been described in detail previously.<sup>14,15</sup> Briefly, endothelial monolayers on coverslips were transduced with AdE-sel and AdS128R-E at a multiplicity of infection (MOI) of 50, incubated for 72 hours at 37°C, and then positioned in a flow chamber mounted under an inverted microscope. In some experiments, HUVEC monolayers were incubated in the presence of RPMI-1640 with a saturating amount of the indicated mAb (10  $\mu$ g/mL) for 20 minutes at 20°C just before the assay. The monolayers were perfused for 5 minutes with perfusion medium and then examined carefully to verify confluence. Indicated leukocytes were then diluted in the perfusion medium to  $10^5$  cells/mL and drawn through the chamber at controlled flow rates to generate a calculated wall shear stress of 1.0 dyne/cm<sup>2</sup> for 10 minutes. The entire period of perfusion was recorded on videotape using a digital video recorder equipped with a time generator. Captured images were then transferred to a PC for image analysis to determine the number of rolling and adherent leukocytes in 5 to 10 randomly selected  $\times 20$  microscope fields during the final minute of each experiment.

### Western Blotting Analysis of MAPK

Endothelial monolayers in 6-well culture plates (Corning) were transduced with either AdE-sel or AdS128R-E at the indicated MOI. After a 72-hour incubation at 37°C, HL60 cells,  $2 \times 10^6$ , were added to the wells, and an adhesion assay under static conditions was carried out as previously described for 10 minutes. After washing with RPMI1640 containing 1% FBS, the monolayers were lysed with an equal volume of 250  $\mu$ L of ice-cold lysis buffer (20 mmol/L HEPES [pH 7.4], 50 mmol/L NaCl, 1% Triton X-100, 20  $\mu$ mol/L leupeptin, 1 mmol/L PMSF, 10  $\mu$ g/mL aprotinin, and 1 mmol/L sodium orthovanadate). After centrifugation at 13 000g for 15 minutes, equal amounts (10  $\mu$ g per lane) of the cell lysates were subjected to Western blotting analysis with anti-ERK1/2, anti-phospho-ERK1/2, anti-p38 MAPK, and anti-phospho-p38 MAPK antibodies. Immunoreactive bands were visualized using horseradish peroxidase-conjugated secondary antibody with an enhanced chemiluminescent system (Amersham Pharmacia Biotech, Buckinghamshire, UK). The activity of ERK1/2 kinase was measured using a p42/44 MAP Kinase Assay Kit (Cell Signaling Technology) according to the manufacturer's protocol. Briefly, active MAPK was immunoprecipitated from HUVEC lysates transduced with AdWT-E or AdS128R-E. The resulting products were then incubated with an Elk-1 fusion protein in the presence of ATP, so that the active MAPK could phosphorylate Elk-1. The amount of phospho-Elk-1 was then determined by Western blotting using a phospho-Elk-1-specific antibody.

### Statistical Evaluation

Data are shown as mean  $\pm$  SD. The distribution of E-selectin allele frequencies was tested by a  $\chi^2$  analysis using a 2 $\times$ 2 table to find associations between MI and the variant allele. All statistical analyses considered  $P < 0.05$  to be statistically significant.

### Results

First we investigated the possible association between an Ser128 to Arg mutation in the E-selectin gene and MI in a Japanese population to elucidate the contribution of this mutation toward the pathogenesis of severe coronary heart disease. One hundred thirty-five patients diagnosed with MI, based on criteria described in the Methods section, were used as subjects, after obtaining informed consent, and their results were compared with those from 325 controls. The S128R mutation of E-selectin was detected using a PCR-restriction fragment length polymorphism analysis of exon 3 of the

**Distribution of E-Selectin Genotype in MI Patients and Controls (%)**

E-Selectin Genotype	MI Patients (n=135)	Control (n=327)
Arg/Arg	0.0	0.0
Arg/Ser	12.6*	6.7
Ser/Ser	87.4	93.2

\*Relative risk=2.0,  $P=0.04$ .  
95% confidential interval=1.04–3.85.

E-selectin gene. We found a significantly ( $P<0.04$ ) increased frequency of Ser128 to Arg mutations in the patient group (17 of 135, 12.6%) compared with the control group (22 of 327, 6.7%), as shown in Table 1. The frequency of E-sel 128Arg-positivity was 11.5% (age at onset equal or younger than 60 years,  $n=73$ , 11%; older than 60 years,  $n=31$ , 12.9%) in male patients, whereas it was 15.6% (age at onset equal or younger than 60 years,  $n=10$ , 20%; older than 60 years,  $n=22$ , 13.6%) in female patients. These findings suggested that the E-sel polymorphism might be a risk factor of MI in the Japanese population, especially in younger females. Furthermore, in accordance with previous reports of an association between this mutation and severe atherosclerosis in a white population,<sup>5,7</sup> these also suggest a strong connection between the E-selectin polymorphism and severe vascular diseases, including MI, in various ethnic groups.

Next, we generated a recombinant adenovirus vector of human E-selectin carrying this mutation and examined its adhesion characteristics in comparison with its WT counterpart using an in vitro flow chamber system. In a previous study by another group,<sup>16</sup> the binding strength of E-selectin to HL60 was reported to be significantly reduced for the mutant (S128R) compared with the WT using transfected COS-7 cells at 4°C. Therefore, we attempted to critically observe the effect of carrying this polymorphism in E-selectin-dependent leukocyte adhesion to vascular endothelium in the presence of flow. We analyzed the surface expression patterns of both the WT (Ad-WT-E) and mutant (Ad-S128R-E) E-selectin in adenoviral-transduced HUVECs using 2 different anti-E-selectin mAbs, 7A9 and H4/18. As shown in Figure 1, the surface expression of the WT was judged to be comparable to mutant E-selectin in the immunoreactivity to these antibodies. Moreover, a fluorescent immunohistochemical analysis of the WT and mutant E-selectin failed to detect any significant difference in their distribution on endothelial surfaces (data not shown).

We then conducted a simulated in vitro flow assay using Ad-WT-E and Ad-S128R-E-transduced HUVEC monolayers. PMNs and PBMNCs from healthy volunteers were isolated for use in flow assays. When PMNs and PBMNCs were perfused at a shear stress of 1 dyne/cm<sup>2</sup>. Ad-S128R-E-transduced HUVECs supported significantly greater levels of rolling and adhesion of PMN than Ad-WT-E-transduced HUVECs (Figures 2A and 2B). Similar levels of enhanced rolling and adhesion were also seen when PBMNCs were used in the assay (Figures 2A and 2B). In contrast, HUVECs transduced with AdRSVLacZ did not exhibit rolling or adhesion of PMNs and PBMNCs (data not shown), which has

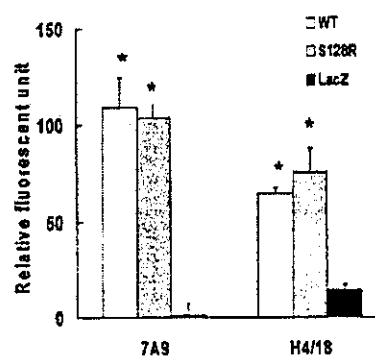


**Figure 1.** Fluorescent immunoassay of HUVECs transduced with WT and variant (S128R) E-selectin adenovirus. HUVECs were plated in 96-well plates and transduced with Ad-WT-E, Ad-S128R-E, or the control (AdRSVLacZ [LacZ]) (MOI=50). HUVEC monolayers were washed twice with 0.1 mL of RPMI1640+1% FBS after adenoviral transduction. Immunoreactive E-selectin was detected with E-selectin-specific mAbs (7A9 or H4/18), as described in the Methods section. Data are representative of 3 separate experiments. \* $P<0.001$  vs AdRSVLacZ-infected HUVECs.

also been previously described.<sup>9,11</sup> Adhesion characterization of the WT and mutant E-selectin were additionally examined at shear stresses of 0.5, 1.0, and 2.0 dyne/cm<sup>2</sup> using HL-60 cells. As shown in Figure 2C, Ad-S128R-E-transduced HUVECs supported significantly greater levels of adhesion under shear stresses of 0.5 and 1.0 dyne/cm<sup>2</sup>. Although not statistically significant, Ad-S128R-E-transduced HUVECs supported greater HL60 cell adhesion compared with those transduced with Ad-WT-E at 2.0 dyne/cm<sup>2</sup>.

To examine the binding characteristics of WT-E and S128R-E selectin, we used the E-selectin adhesion blocking mAb (7A9) on PMN adhesion to WT-E and S128R-E-selectin-transduced HUVEC. As shown in Figure 3, pretreatment of Ad-WT-E-transduced HUVECs with 7A9 significantly blocked PMN rolling (77.5±42% inhibition versus control IgG,  $n=8$ ,  $P<0.003$ ) as well as adhesion (87.0±7.7% inhibition,  $n=8$ ,  $P<0.0001$ ), whereas pretreatment of Ad-S128R-E-transduced HUVECs with 7A9 partially blocked PMN rolling (46.7±16.7% inhibition,  $n=7$ ,  $P<0.003$ ) and adhesion (51.0±9.6% inhibition,  $n=7$ ,  $P<0.0009$ ). These results suggest that the S128R substitution in E-selectin dramatically conferred a ligand-binding affinity to E-selectin.

In addition to mediating leukocyte adhesion to vascular endothelium, recent studies have indicated that E-selectin may also transmit outside-in signals in vascular endothelium during leukocyte-endothelial interactions.<sup>9,17</sup> Hu et al<sup>18</sup> recently reported that E-selectin-dependent leukocyte adhesion induced activation of the MAPK pathway. To explore the functional significance of the S128R polymorphism in E-selectin-dependent signaling, Western blotting analysis was carried out using lysates prepared from HUVECs transduced with Ad-WT-E or Ad-S128R-E-selectin, and the phosphorylation of ERK and p38 MAPK was examined. As shown in Figures 4A and 4B, Ad-S128R-E-transduced HUVECs exhibited a constitutive phosphorylation of ERK and p38 MAPK kinase that was not observed in Ad-WT-E-transduced HUVECs. Adhesion of HL60, a leukocyte cell

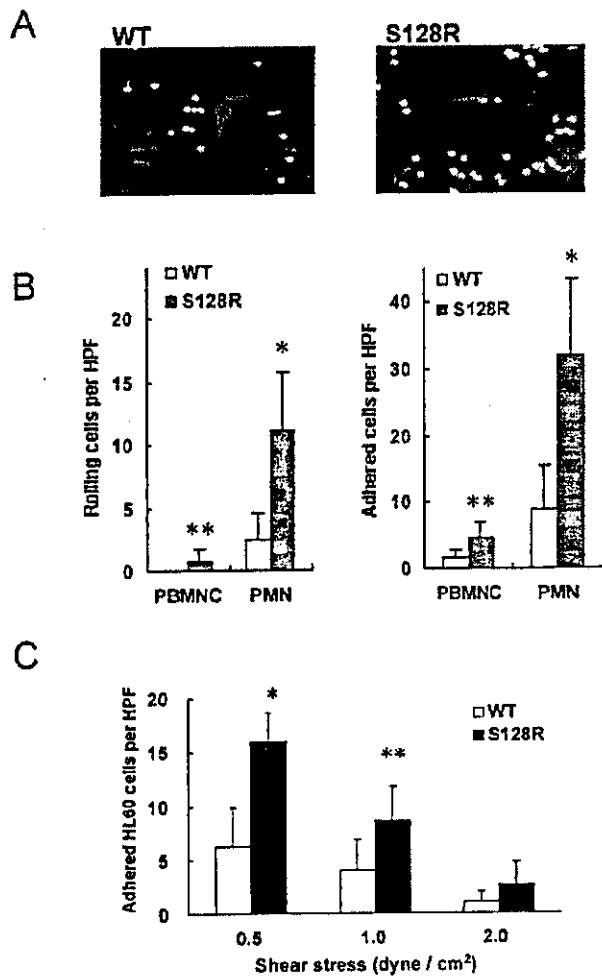


**Figure 2.** Adhesive interactions of HL60 cells, U937 cells, PBMC, and PMN on HUVECs transduced with WT and variant (S128R) E-selectin adenovirus under flow conditions. HUVEC monolayers were transduced with Ad-WT-E or Ad-S128R-E (MOI=50). A, Representative micrographs of PMN adhesion to Ad-WT-E (WT) or Ad-S128R-E (S128R) transduced HUVEC monolayer under flow (shear stress=1.0 dyn/cm<sup>2</sup>). Magnification,  $\times 200$ . B, Quantitated PMN and PBMC adhesion ( $1 \times 10^5$ /mL) to AdWT-E (WT) or AdS128R-E (S128R) transduced HUVEC monolayers under flow (shear stress=1.0 dyn/cm<sup>2</sup>). The numbers of rolling and adhered cells were calculated as described in the Methods section. Data are representative of the results of 4 separate experiments. \* $P < 0.005$  vs WT; \*\* $P < 0.05$  vs WT. C, Adhesion of HL60 cells ( $1 \times 10^5$ /mL) to AdWT-E (WT) or AdS128R-E (S128R) transduced HUVEC monolayers was examined under various levels of shear stress (0.5, 1.0, and 2.0 dyn/cm<sup>2</sup>). Data are representative of the results of two separate experiments. \* $P < 0.0005$  vs WT; \*\* $P < 0.005$  vs WT.

line possessing the E-selectin ligand, to HUVECs significantly induced the phosphorylation of ERK and p38 MAPK in Ad-WT-E-transduced HUVECs but not in Ad-S128R-E-transduced HUVECs (Figures 4A and 4B). This enhanced phosphorylation was observed in proportion to the virus titer and E-selectin expression levels (data not shown), suggesting that the constitutive activation of MAPK was an S128R polymorphism-dependent phenomenon. Moreover, direct measurement of ERK kinase activity, as shown in Figure 5,

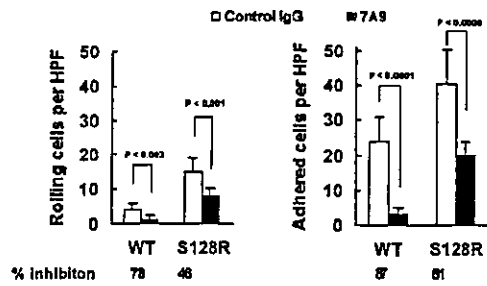


**Figure 3.** Effect of antibodies against E-selectin on PMN adhesion to WT and mutant (S128R) E-selectin-transduced HUVECs under flow conditions. HUVEC monolayers were transduced with AdWT-E or AdS128R-E at an MOI of 50. A, HUVEC monolayers were incubated in the presence of an anti-E-selectin monoclonal antibody, 7A9, or the control IgG for 20 minutes before the adhesion assay under flow conditions using isolated PMN ( $1 \times 10^5$ /mL). Data are expressed as the percentage of the number of PMN adhesions seen with 7A9-treated HUVECs to that of the control IgG-treated HUVECs. Data are representative of the results of 3 separate experiments.

revealed a significantly greater quantity of phosphorylated-Elk-1 protein detected from Ad-S128R-E-transduced HUVECs compared with those transduced with Ad-WT-E in the absence of HL60. In addition, HL60-induced enhancement of ERK kinase activity, as observed in Ad-WT-E-transduced HUVECs, was not observed in Ad-S128R-E-transduced HUVECs (Figure 5).

### Discussion

Genetic mutations and polymorphisms are known to be risk factors for atherosclerosis and have been extensively studied for their potential association with atherogenic vascular diseases. Similarly, mutations in adhesion molecules, including P-selectin<sup>19</sup> and E-selectin,<sup>5</sup> and their association with cardiovascular diseases have recently been investigated. In the present study, we demonstrated that a Serine128Arg mutation in the EGF domain of E-selectin is a potential risk factor for genetic susceptibility to MI in the Japanese population. Considering the possibility of selection bias, which may have an influence on the results of association studies, we carefully examined the genetic and ethnic homogeneity of our study population along with the competency of the control group. Our entire study population resided in Tokyo and adjacent areas within Japan, where individuals are considered to have a homogeneous genetic background. Furthermore, the distribution of the E-selectin genotype in our control group showed Hardy-Weinberg equilibrium, which verified that the control group was statistically appropriate.

In a study of the association between the E-selectin gene and atherosclerotic vascular diseases, Ye et al<sup>6</sup> reported that the Ser128Arg mutation was associated with coronary artery disease in their patients. Wenzel et al<sup>7</sup> also found that both the Ser128Arg and Leu554Phe mutations in the transmembrane domain were related to early severe atherosclerosis in a German population. Results of these studies, conducted using subjects with different ethnic and genetic backgrounds, suggest the possibility that mutations found in the E-selectin gene (Ser128Arg and Leu554Phe) may play a functional role

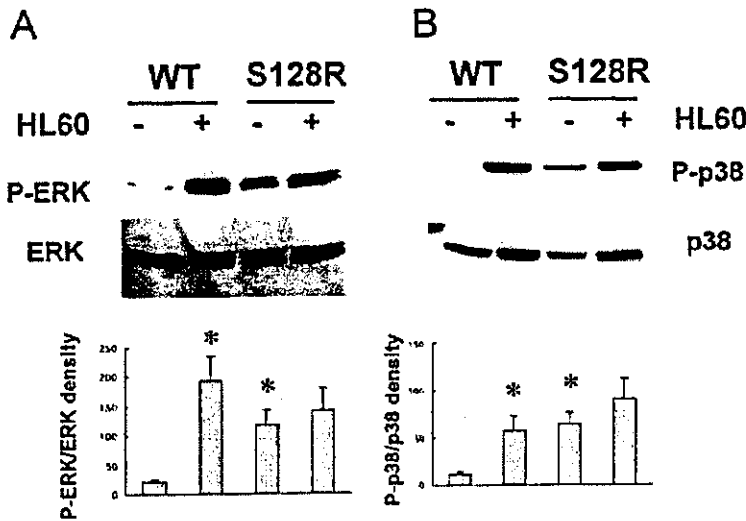


**Figure 4.** HUVECs in 6-well culture plates were transduced with AdWT-E (WT) or AdS128R-E (S128R) at an MOI of 50. Seventy-two hours after adenoviral transduction, the monolayers were incubated in the presence (+) or absence (-) of HL60 cells ( $2 \times 10^6$ /well) for 10 minutes. After washing nonadhered HL60 cells, cell lysates were prepared as described in the Methods section. A, ERK and phosphorylated (P-) ERK; B, p38 MAPK and phosphorylated (P-) p38 MAPK expressions were detected by Western blotting analysis (10  $\mu$ g protein/lane). Bar graph represents the percentage of density of the phosphorylated band to that of the total protein band. \* $P < 0.05$  vs WT (-). Blots are representative of 3 independent experiments.

in the development of atherosclerosis. Notably, recent findings have also demonstrated that the association between the E-selectin S128R polymorphism and coronary artery calcification was prominent among younger women.<sup>20</sup> We also previously demonstrated that the relationship between the E-selectin S128R polymorphism and MI was much stronger in women younger than 60 years of age.<sup>21</sup> Together, these findings may indicate that an altered expression of E-selectin counteracts the inhibitory effects of estrogens to reduce the expression of adhesion molecules. Thus, as a coronary risk

factor, the E-selectin S128R polymorphism may be of particular importance for younger women.

To functionally examine this issue, we created an experimental model that used vascular endothelium that overexpressed mutant E-selectin via a recombinant adenovirus. We found that the Ser128Arg mutation of E-selectin significantly enhanced its adhesion to leukocytes under physiological flow conditions, in contrast to Wentzel et al,<sup>16</sup> who demonstrated that the Ser128Arg polymorphism reduces E-selectin binding to HL60 cells using COS-7 transfectants at 4°C. Our results make an interesting comparison to theirs, and we cannot exclude the differences seen in the expression profiles of the adhesion molecules and intracellular cytoskeleton between COS-7 cells and HUVECs, although the differences in assay conditions (static adhesion assay at 4°C versus physiological flow conditions at 37°C) may have had an influence.

It has also been reported that the Ser128Arg mutation totally confers carbohydrate specificity to E-selectin,<sup>8</sup> and we also demonstrated such an effect by an anti-E-selectin mAb in Ser128Arg mutant E-selectin-transduced HUVECs in the present study. The inhibitory effect of the anti-E-selectin mAb on S128R mutant E-selectin-dependent PMN adhesion to HUVECs was not as dramatic as that on HUVEC transduced with its WT counterpart, although it was significant. Moreover, although E-selectin participates primarily in PMN adhesion rather than PBMNC adhesion to vascular endothelium, the S128R-E-selectin-transduced HUVEC exhibited a significantly greater level of PBMNC rolling and adhesion than the WT-E-selectin-transduced HUVEC under flow conditions (Figure 2B). These data also strongly indicate an altered ligand specificity of S128R-E-selectin.

The mechanism by which this mutation causes enhanced binding activity under flow requires additional study. However, as revealed by a three-dimensional crystal-structural analysis of E-selectin, we now know that the position of the 128th amino acid in the EGF domain of E-selectin does not allow it to directly participate in the ligand-binding pocket.

Recent observations suggest that the polymorphisms found in cell-surface receptors lead to a constitutive activation of the receptors in the absence of their ligands,<sup>22,23</sup> possibly

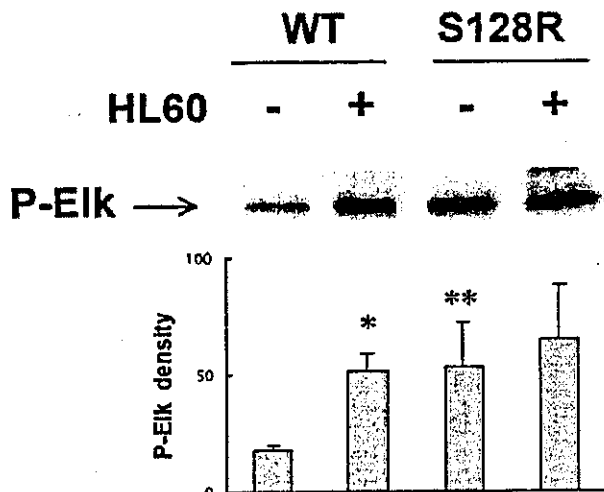


**Figure 5.** ERK protein was constitutively activated in HUVECs transduced with variant (S128R) E-selectin but not WT E-selectin. Endothelial monolayers in 6-well culture plates were transduced with AdWT-E or AdS128R-E at an MOI of 50. Seventy-two hours after adenoviral transduction, the monolayers were incubated in the presence (+) or absence (-) of HL60 cells ( $2 \times 10^6$ /well) for 10 minutes. After washing the nonadhered HL60 cells, cell lysates were prepared as described in the Methods section. Activated forms of ERK were immunoprecipitated, and their activities assessed by the phosphorylation of EIK, a potent substrate of ERK kinase. Bar graph represents the density of the bands expressed in arbitrary densitometry units. \* $P < 0.05$  vs WT (-); \*\* $P < 0.05$  vs WT (-). Blots are representative of 3 independent experiments.